Search for long-lived heavy neutral leptons with lepton flavour conserving or violating decays to a jet and a charged lepton

The CMS collaboration

E-mail: cms-publication-committee-chair@cern.ch

ABSTRACT: A search for long-lived heavy neutral leptons (HNLs) is presented, which considers the hadronic final state and coupling scenarios involving all three lepton generations in the 2–20 GeV HNL mass range for the first time. Events comprising two leptons (electrons or muons) and jets are analyzed in a data sample of proton-proton collisions, recorded with the CMS experiment at the CERN LHC at a centre-of-mass energy of 13 TeV, corresponding to an integrated luminosity of 138 fb^{-1}. A novel jet tagger, based on a deep neural network, has been developed to identify jets from an HNL decay using various features of the jet and its constituent particles. The network output can be used as a powerful discriminating tool to probe a broad range of HNL lifetimes and masses. Contributions from background processes are determined from data. No excess of events in data over the expected background is observed. Upper limits on the HNL production cross section are derived as functions of the HNL mass and the three coupling strengths $V_{\ell N}$ to each lepton generation ℓ and presented as exclusion limits in the coupling-mass plane, as lower limits on the HNL lifetime, and on the HNL mass. In this search, the most stringent limit on the coupling strength is obtained for pure muon coupling scenarios; values of $|V_{\mu N}^2| > 5\,(4) \times 10^{-7}$ are excluded for Dirac (Majorana) HNLs with a mass of 10 GeV at a confidence level of 95% that correspond to proper decay lengths of 17 (10) mm.

Contents

1 Introduction

The observation of neutrino oscillations [1–3], a mechanism by which neutrinos can change their flavour, implies that at least two of the standard model (SM) neutrinos must have a nonzero mass and that neutral lepton flavour number is not a conserved quantity. Upper limits on the sum of all neutrino masses have been derived from cosmological considerations, whereas the study of particle decays via charged currents (e.g. β-decay of tritium [4]) has allowed upper limits to be set on the mass per lepton generation [5]. The smallness of the neutrino masses compared to those of the other SM particles and to the vacuum expectation value of the Higgs potential suggests that there might exist another mechanism, beyond the SM, to explain the fundamental nature of neutrinos.

In this context, a minimal extension to the SM is given by a "seesaw" mechanism [6–11], which postulates additional neutral leptons that are singlets with respect to the SM gauge groups and hence can possess an arbitrary mass. Through coupling to the Higgs field, these new particles mix with the SM neutrinos after electroweak symmetry breaking. The resulting mass eigenstates correspond to the three SM neutrinos with small masses and to three nearly sterile heavy neutral leptons (HNLs) that couple to the W and Z bosons in a similar way as the SM neutrinos. However, their coupling strengths are suppressed because of small mixing angles. An overview of the phenomenology of HNLs at the GeV mass scale can be found in ref. [12].

A common model that incorporates HNLs via the seesaw mechanism is the neutrino minimal standard model [13, 14]. Models incorporating HNLs are further motivated since, beside neutrino oscillations, they can explain additional phenomena that are not described by the SM: the baryonic asymmetry of the universe and the nature of dark matter [15, 16]. Phenomenologically, an HNL can be either a Dirac or Majorana particle, N, that is characterized by its mass m_N and coupling strengths V_{eN}, $V_{\mu N}$, and $V_{\tau N}$ to electrons, muons, and tau leptons, respectively. The HNL can be long-lived for sufficiently low coupling strengths since its partial three-body decay widths are proportional to $m_N^5 |V_{\ell N}|^2$, where $\ell \in \{e, \mu, \tau\}$ [12]. In general, lepton flavour number is not a conserved quantity in HNL interactions. It is only conserved in the special case where only one $V_{\ell N}$ coupling is nonzero.

Searches for HNLs are pursued at various experiments covering a wide range of masses from a few keV up to several TeV [17, 18]. At the CERN LHC, searches for HNLs are performed employing their production in the decay of mesons or through on-shell W or Z bosons, where the most stringent limits on V_{eN} and $V_{\mu N}$ can be derived starting at the GeV mass scale. Corresponding analyses have been conducted by the ATLAS, CMS, and LHCb Collaborations [19–32], which mainly target signatures arising from the production of HNLs and their prompt decay to only one lepton generation (e or μ), whereas long-lived HNLs and the possibility of cross-generation lepton couplings are only recently being explored. Various of these experimental results have been statistically combined using the GAMBIT tool [33].

The two most common three-body decay modes of HNLs involve a virtual W boson and result in final states comprising two leptons and a neutrino or one lepton and two quarks with branching fractions of approximately 25 and 50% for $m_N > 5\,\mathrm{GeV}$, respectively. A signature considered in this search is depicted in figure 1, which shows the Feynman diagram for Dirac HNL production at the LHC via an on-shell W boson for $m_N < m_W$, and the subsequent HNL decay to a lepton and two quarks. Alternatively, HNLs can also be produced in decays of b hadrons for $m_N < m_b$ at the LHC, which is not considered in this search. For long-lived HNLs, the decay products are spatially separated (i.e. displaced) from the point where the HNL is produced. Thus, the process depicted in figure 1 results in a signature comprising one prompt lepton ℓ_1, a displaced lepton ℓ_2, and at least one displaced jet $j^\star$, a collimated set of particles originating from the hadronization of the two quarks. If the HNL is highly Lorentz-boosted, a single jet can also be formed encapsulating all displaced decay products from the HNL, a case that is also considered in this analysis. For Dirac HNLs, the final-state leptons have opposite electrical charges, while for Majorana HNLs they can have either the same or opposite electrical charges with equal probability.

In this paper, a search for long-lived Dirac and Majorana HNLs is performed without assuming that their coupling is exclusive to only one lepton generation. Instead, HNL production is investigated in the full coupling space spanned by V_{eN}, $V_{\mu N}$, and $V_{\tau N}$ for $2 < m_N < 20\,\mathrm{GeV}$, where an HNL proper lifetime τ_0 of up to $c\tau_0 = 10^4\,\mathrm{mm}$ can be probed. A data set of proton-proton (pp) collisions recorded by the CMS detector at a centre-of-mass energy of 13 TeV and corresponding to an integrated luminosity of $138\,\mathrm{fb}^{-1}$ is analyzed. Events containing two leptons (e or μ) and jets are selected to target the hadronic HNL decay channel. Several event categories are defined to provide sensitivity to Dirac and Majorana HNL signals, both prompt and displaced, while contributions from background processes
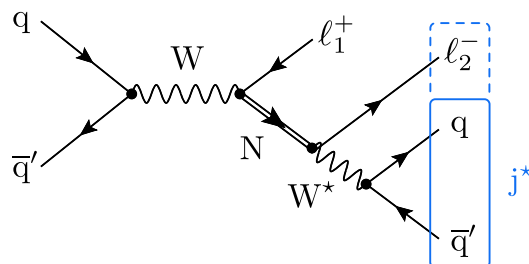
Figure 1. Born-level Feynman diagram for Dirac HNL production and decay via a charged-current interaction. Corresponding diagrams exist also for Dirac anti-HNL and Majorana HNL production and decay. In this search, the HNL decay products, encapsulated by the boxes, can be found collimated within a single jet $j^\star$.

are estimated from data. A central feature of the analysis is the identification of displaced jets (with or without an overlapping displaced lepton) using a deep neural network (DNN) that does not explicitly require the reconstruction of displaced vertices. The DNN uses a domain adaptation technique to ensure accurate performance of the resulting classifier in data. The presented search explores an orthogonal phase space compared to ref. [28], where similar parameter ranges in m_N and $c\tau_0$ are probed but events with three leptons and no jets have been investigated instead.

An outline of the paper is as follows: a brief description of the CMS detector and the reconstruction of events is given in section 2. The real and simulated data sets are detailed in section 3, followed by a description of the event selection and categorization in section 4. In section 5, details of the identification of displaced jets based on a DNN are presented including its architecture and training setup. The determination of the number of events from background processes is described in section 6. A list of the sources of systematic uncertainties affecting the expected number of signal and background events can be found in section 7. The results are presented in section 8, followed by a summary in section 9.

Tabulated results are provided in the HEPData record for this analysis [34].

2 The CMS detector and event reconstruction

The central feature of the CMS apparatus is a superconducting solenoid of 6 m internal diameter, providing a magnetic field of 3.8 T. Within the solenoid volume are a silicon pixel and strip tracker, a lead tungstate crystal electromagnetic calorimeter (ECAL), and a brass and scintillator hadron calorimeter (HCAL), each composed of a barrel and two endcap sections. Forward calorimeters extend the pseudorapidity η coverage provided by the barrel and endcap detectors. Muons are detected in gas-ionization chambers embedded in the steel flux-return yoke outside the solenoid. A more detailed description of the CMS detector, together with a definition of the coordinate system used and the relevant kinematic variables, can be found in ref. [35].

The particle-flow (PF) algorithm [36] aims to reconstruct and identify each individual particle in an event, with an optimized combination of information from the various elements of the CMS detector. The energy of photons is obtained from the ECAL measurement.

The energy of electrons is determined from a combination of the electron momentum at the primary interaction vertex as determined by the tracker, the energy of the corresponding ECAL cluster, and the energy sum of all bremsstrahlung photons spatially compatible with originating from the electron track. The energy of muons is obtained from the curvature of the corresponding track. The energy of charged hadrons is determined from a combination of their momentum measured in the tracker and the matching ECAL and HCAL energy deposits, corrected for the response function of the calorimeters to hadronic showers. Finally, the energy of neutral hadrons is obtained from the corresponding corrected ECAL and HCAL energies. The PF algorithm is able to reconstruct electrons and muons with efficiencies of about 80 and 95%, respectively, for transverse displacements of less than 1 cm. At larger displacements, the efficiencies gradually reduce and approach zero at 40 cm and 1 m, respectively, as determined from simulation.

The missing transverse momentum vector $\vec{p}_T^{\text{miss}}$ is defined as the projection onto the plane perpendicular to the beams of the negative vector momentum sum of all PF candidates in an event. Its magnitude is referred to as p_T^{miss}. Jets are reconstructed from PF candidates and clustered by applying the anti-k_T algorithm [37] with a distance parameter of 0.4. The reconstruction of jets is fully efficient with transverse displacements up to the edge of the inner tracking volume. After this, the reconstruction efficiency degrades as displaced charged particles can only be identified through their calorimetric energy deposits.

The primary vertex (PV) is taken to be the vertex corresponding to the hardest scattering in the event, evaluated using tracking information alone, as described in section 9.4.1 of ref. [38].

Events with spuriously high p_T^{miss}, originating from a variety of reconstruction failures, detector malfunctions, or noncollision backgrounds, are vetoed by event filters with negligible impact on events with genuine p_T^{miss} [39].

Events of interest are selected using a two-tiered trigger system. The first level, composed of custom hardware processors, uses information from the calorimeters and muon detectors to select events at a rate of around 100 kHz within a fixed latency of 4 μs [40]. The second level, known as the high-level trigger, consists of a farm of processors running a version of the full event reconstruction software optimized for fast processing, and reduces the event rate to around 1 kHz before data storage [41].

3 Data set and simulated samples

The analyzed sample of pp collision data was recorded at $\sqrt{s} = 13$ TeV with the CMS detector during 2016, 2017, and 2018. The subsamples by year correspond to integrated luminosities of 36.3, 41.5, and 59.7 fb^{-1}, respectively. The 2016, 2017, and 2018 data sets are analyzed independently and only combined for the final result to account for differences related to the data-taking conditions and to apply proper corrections and calibrations per year. Events were triggered by requiring at least one electron or muon candidate within $|\eta| < 2.4$. Electron candidates must have a transverse momentum p_T of at least 27 (32) GeV in 2016 (2017, 2018), and pass additional identification requirements [42]. Muon candidates have to fulfil $p_T > 24$ GeV (2016, 2018) or $p_T > 27$ GeV (2017), and have to be isolated from other activity in the event [43].

Samples of simulated signal events are used to evaluate the detector resolution, efficiency, and acceptance for HNL production processes. Additionally, samples of simulated background events are used for understanding the composition of the data and to optimize the analysis strategy. Samples of simulated events are furthermore used to train machine learning algorithms. However, the final results are obtained by determining the contribution from background processes using data in sideband regions.

Samples of HNL production with various values of m_N ranging from 2 to 20 GeV, and with $10^{-5} < c\tau_0 < 10^4$ mm, are generated in the five-flavour scheme at leading order (LO) accuracy (i.e. tree-level) using the MADGRAPH5_AMC@NLO v2.6.5 event generator [44]. The parton distribution function (PDF) set used is NNPDFv3.1 [45]. Parton showering is performed with PYTHIA 8.230 [46] using the underlying event tunes CUETP8M1 [47] (2016) or CP5 [48] (2017, 2018). Each sample is generated assuming an equal coupling strength for the three lepton generations, $V_{eN} = V_{\mu N} = V_{\tau N}$. The resulting events are reweighted to also probe different combinations of coupling strengths. For these, the HNL displacement, determined by the total HNL decay width Γ_N, has to be kept constant such that the subsequent detector simulation and event reconstruction do not need to be rerun. The HNL decay width can be written as

$$\Gamma_N(m_N, V_{eN}, V_{\mu N}, V_{\tau N}) = \underbrace{A_e(m_N)|V_{eN}|^2}_{=\Gamma_e} + \underbrace{A_\mu(m_N)|V_{\mu N}|^2}_{=\Gamma_\mu} + \underbrace{A_\tau(m_N)|V_{\tau N}|^2}_{=\Gamma_\tau}, \qquad (3.1)$$

where the factors A_ℓ, calculated by MADGRAPH5_AMC@NLO, describe the dependence of the partial widths per lepton flavour Γ_ℓ on m_N. Equation (3.1) describes an ellipsoid spanned by V_{eN}, $V_{\mu N}$, and $V_{\tau N}$ for a given Γ_N and m_N. Thus, the generated events of a particular sample can be reweighted to any coupling combination on the ellipsoid surface. The barycentric coordinates f_e, f_μ, and f_τ with $\sum f_\ell = 1$ are introduced, which denote the relative ratios between the coupling strengths squared $|V_{eN}|^2 : |V_{\mu N}|^2 : |V_{\tau N}|^2 \equiv f_e : f_\mu : f_\tau$. In total, 66 equidistant weights in f_ℓ space are used, which have been calculated by the event generator at the matrix element level [49]. The modelling of low-p_T jets originating from HNL decays has been validated by using the average charged particle multiplicity and comparing it to previous measurements in e^+e^- annihilation [50]. The HNL production cross sections are calculated at next-to-leading order (NLO) in the strong coupling constant, using the same generator settings, and are found to be approximately 10% higher than the cross sections calculated at tree level for all samples.

Further details on the HNL Lagrangian and the implementation of models for both Dirac and Majorana HNLs can be found in refs. [51–54].

The major background processes are the production of vector bosons in association with jets (W+jets, Z/γ^*+jets, and $V\gamma^*$+jets, where $V \in \{W, Z\}$), top quark production ($t\bar{t}$, single t), and multijet events consisting of jets produced through the strong interaction. Samples of simulated background events are generated at NLO accuracy using the MADGRAPH5_AMC@NLO or POWHEG [55–57] 2.0 event generators with the exception of multijet events that are generated at LO with PYTHIA. The NNPDFv3.1 set is used and parton showering is performed by PYTHIA with the same underlying event tunes as used for the signal samples.

The simulated events are overlaid with additional simulated minimum bias collisions ("pileup") according to the distributions inferred from the data per year. All generated events undergo a full GEANT4 [58] simulation of the detector response and are subjected to the same event reconstruction as the data.

4 Event selection and categorization

Events containing two leptons ($\ell \in \{e, \mu\}$) and at least one jet are analyzed. This signature targets the production and decay of HNLs via charged currents, $\text{pp} \to \ell_1 \text{N}$, $\text{N} \to \ell_2 \text{q}\overline{\text{q}}'$. The first lepton ℓ_1 is expected to originate from the production vertex, while the second lepton ℓ_2 and the jet(s) from the hadronization of the two quarks can be displaced with respect to the PV. The hadronic HNL decay channel targeted by this analysis has a branching fraction of about 50% for $m_\text{N} > 5\,\text{GeV}$, which is approximately twice as large compared to the leptonic decay channel, $\text{N} \to \ell^\pm \ell^\mp \nu$. Other decay channels occur via neutral currents and result in $\nu \text{q}\overline{\text{q}}$ or $\nu \nu \overline{\nu}$ final states. Decays to other BSM particles, e.g. lighter HNLs, are not considered in the model used for generating the signal samples. In scenarios where $m_\text{N} \lesssim 8\,\text{GeV}$, the HNL is found to be sufficiently Lorentz-boosted with respect to the laboratory frame such that its decay products are collimated inside a single jet. The selected events also include leptonic τ decays to e or μ. Tau lepton decays to hadrons are not considered in this analysis because efficient event trigger strategies with sufficiently low p_T thresholds on τ candidates were not available. In the following, the selection criteria for the physics objects are described.

4.1 Physics object selection

Two types of candidates are defined for electrons and muons depending on whether they are considered for ℓ_1 or ℓ_2. The former is used to trigger the event and thus has to fulfil more stringent, tight identification criteria, while the latter is required to pass only relaxed, loose identification criteria instead. This increases the signal selection efficiency in cases when ℓ_2 is displaced and/or clustered inside a jet.

Tight electron candidates are required to have a p_T of at least $29\,(34)\,\text{GeV}$ and be within $|\eta| < 2.4$ for the 2016 (2017, 2018) data-taking periods. A boosted decision tree (BDT) discriminant is used to identify genuine electrons with an efficiency of $\approx 90\%$ as measured in Drell-Yan events [42]. This BDT is trained using several features of the electron track and of the associated energy deposits in the ECAL, including the relative isolation parameter $I_\text{rel}(\text{e})$. This parameter is defined as the scalar p_T sum of the charged and neutral PF candidates within a cone of radius $\Delta R = \sqrt{(\Delta\eta)^2 + (\Delta\phi)^2} = 0.3$ around the electron candidate, excluding the candidate itself, divided by the electron p_T. Here, $\Delta\eta$ and $\Delta\phi$ are, respectively, the pseudorapidity and azimuthal angle measured in radians and relative to the electron direction. The relative contribution from pileup is estimated as $A_\text{eff}\,\rho$ and subtracted from the isolation parameter, where A_eff denotes an η-dependent effective area, and ρ is the median of the transverse energy density in a $\delta\eta$-$\delta\phi$ region calculated using the charged particle tracks associated with the pileup vertices. Furthermore, the electron candidate has to originate from the vicinity of the PV by requiring a transverse and longitudinal impact parameter of $|d_\text{xy}| < 0.05\,(0.10)\,\text{cm}$ and $|d_\text{z}| < 0.1\,(0.2)\,\text{cm}$, respectively, in the ECAL barrel (endcap) region.

Loose electron candidates need to fulfil $p_T > 5\,\mathrm{GeV}$, $|\eta| < 2.4$, and pass a series of loose selection criteria that have been optimized to enhance the acceptance for displaced electrons that can also be clustered within nearby jets, as defined below. The criteria are a modified version of the standard identification requirements [42] but allow for any number of missing electron track hits in the inner tracker. Furthermore, no requirements on the compatibility with the PV or on $I_{\mathrm{rel}}(\mathrm{e})$ are imposed.

Tight muon candidates must be within $|\eta| < 2.4$, have a p_T of at least 26, 29, 26 GeV for the 2016, 2017, 2018 data-taking periods, respectively, and fulfil additional identification requirements optimized for the selection of genuine muons that result in efficiencies of $>96\%$ as determined from a data sample of Drell-Yan events [59]. In particular, muon candidates are required to be within $|d_{\mathrm{xy}}| < 0.01\,\mathrm{cm}$ and $|d_z| < 0.05\,\mathrm{cm}$ of the PV. Furthermore, the candidates must be isolated with a relative isolation parameter $I_{\mathrm{rel}}(\mu) < 15\%$, which is defined as the scalar p_T sum of PF photons and charged and neutral PF hadrons within a cone of radius of $\Delta R = 0.4$, divided by the muon p_T. Contributions from pileup are estimated from the energy deposited by charged hadrons within the isolation cone that are associated with pileup vertices and subtracted from the isolation parameter.

Loose muon candidates are required to pass $p_T > 3\,\mathrm{GeV}$, $|\eta| < 2.4$, and fulfil only minimal requirements necessary for being reconstructed by the PF algorithm [59]. Similar to loose electron candidates, loose muon candidates are allowed to be inside jets and do not have to be compatible with the PV.

Events with exactly two leptons of any charge and flavour combination are considered for further analysis, where at least one needs to fulfil the tight candidate requirements. This results in event categories, denoted "$\ell_1\ell_2$", where the first lepton is the tight candidate that is also matched to a corresponding event trigger and has to have $p_T(\ell_1) > p_T(\ell_2)$ to avoid the double counting of events where both leptons are responsible for a positive decision by the trigger system.

The momentum of each jet is defined as the vectorial momentum sum over all its constituent PF candidates. To mitigate the contribution of additional tracks and calorimetric energy depositions from pileup interactions, PF candidates identified as originating from pileup vertices are discarded and an offset correction is applied to account for remaining contributions [60]. Jet energy corrections are derived from simulation so that their average measured energy becomes identical to that of particle level jets. In situ measurements of the momentum balance in dijet, photon+jet, Z+jet, and multijet events are used to determine any residual differences between the jet energy scale in data and in simulation, and appropriate corrections are made. The corrections are propagated to the measured $\vec{p}_T^{\mathrm{miss}}$.

The analysis considers jets within $|\eta| < 2.4$ with a calibrated p_T greater than 20 GeV. Jets that overlap with ℓ_1 within $\Delta R < 0.4$ are ignored, whereas the jet p_T needs to be at least 30 GeV if ℓ_2 is within $\Delta R < 0.4$ from the jet. Jets close to ℓ_2 are also ignored if $I_{\mathrm{rel}}(\ell_2) < 15\%$ to reject jets that are primarily clustered from isolated leptons. The jet that is the closest in ΔR to ℓ_2 is interpreted as the jet from the (displaced) HNL decay and is hereafter referred to as $\mathrm{j}^\star$. In simulation this procedure assigns a reconstructed jet correctly to the HNL decay with an efficiency of larger than 95%. Events with more than one displaced jet from the HNL decay passing the event selection constitute a negligible fraction and are hence not explicitly targeted by the selection.

4.2 Event categories

The invariant mass $m_{\ell\ell j^\star}$ is calculated from the summed four momenta of the two leptons and $j^\star$. In signal events, $m_{\ell\ell j^\star}$ approximates the mass of the W boson. The signal region (SR) is defined for selected events with an invariant dilepton mass of $20 < m_{\ell\ell} < 80\,\text{GeV}$, $p_{\text{T}}^{\text{miss}} < 60\,\text{GeV}$, and consisting of 1–4 jets, to reject Z/γ^*+jets, W+jets, and high-p_{T} processes (e.g. $\text{t}\bar{\text{t}}$) with many jets that can additionally be produced in association with neutrinos. Additionally, $j^\star$ must be within $\Delta R < 1.3$ of ℓ_2 since in signal events both are expected to be spatially close together and even overlap when the HNL is sufficiently boosted. To suppress contributions from low-p_{T} leptons produced during hadronization, which are often found in W+jets and multijet events, the ratio $p_{\text{T}}(j^\star)/p_{\text{T}}(\ell_2)$ must be smaller than 2–4 depending on the data-taking period and category, since the p_{T} threshold for leptons also varies per data-taking period. Additionally, $\mu^\pm\mu^\mp$ events must have $m_{\ell\ell} < 70\,\text{GeV}$ to further reject the overwhelming Z/γ^*+jets background in these categories. After applying all object and event selection criteria, the following approximate fractions of signal events remain when summed over all lepton flavour combinations: 2.5% for $c\tau_0 \leq 1\,\text{mm}$, 1.5% for $c\tau_0 = 10\,\text{mm}$, 0.9% for $c\tau_0 = 100\,\text{mm}$, and less than 0.1% for scenarios with larger $c\tau_0$ values. These low efficiencies are primarily due to HNLs decaying into low-p_{T} leptons that often do not satisfy the p_{T} thresholds applied as part of the event selection.

A control region (CR), enriched in background events (mainly Z/γ^*+jets), is obtained by inverting the SR selection on $m_{\ell\ell}$, i.e. to be larger than $80\,\text{GeV}$. This region is used for validating various aspects of the analysis strategy such as the modelling of the simulation and the displaced jet tagger (section 5).

Events in the SR are categorized through a series of criteria to be simultaneously sensitive to various HNL mass and coupling scenarios. First, events are separated depending on the lepton flavour combination (ee, eμ, μe, $\mu\mu$) for probing different coupling scenarios and on the lepton charge combination, i.e. opposite- or same-sign (OS, SS) events, to be sensitive to Dirac and Majorana HNL production, simultaneously. Furthermore, events are classified as either "boosted" if ℓ_2 overlaps with $j^\star$ (i.e. $\Delta R < 0.4$) or "resolved" otherwise. Finally, events are split into three subcategories depending on the significance of the transverse displacement $d_{\text{xy}}^{\text{sig}}$ of ℓ_2 with respect to the PV; $d_{\text{xy}}^{\text{sig}}$ is defined as $d_{\text{xy}}/\sigma_{\text{xy}}$, where d_{xy} and σ_{xy} are the transverse impact parameter and its uncertainty, respectively, as determined by the lepton track fit. The $d_{\text{xy}}/\sigma_{\text{xy}}$ parameter is chosen because potential mismeasurements in d_{xy} and σ_{xy} cancel each other out in the ratio and its distribution in the CR is found to be well described by the simulation. Events are grouped by the $d_{\text{xy}}^{\text{sig}}$ values into prompt-like ($d_{\text{xy}}^{\text{sig}} < 3$), displaced ($3 < d_{\text{xy}}^{\text{sig}} < 10$), and very displaced ($d_{\text{xy}}^{\text{sig}} > 10$) subcategories that probe a wide range of HNL lifetime scenarios. In total, this results in 48 independent event categories.

Distributions of $m_{\ell\ell j^\star}$ in the SR are presented in figure 2 for events with OS and SS lepton pairs. The data are found to be described well by the prediction from simulation normalized to the integrated luminosity. A representative signal scenario for Majorana HNL production assuming $m_{\text{N}} = 10\,\text{GeV}$ and $c\tau_0 = 1\,\text{mm}$ with $V_{\text{eN}} = V_{\mu\text{N}} = V_{\tau\text{N}}$ is overlaid. A resonance is expected in the $m_{\ell\ell j^\star}$ distribution for signal events at the W boson mass, while a broader spectrum is found for background processes. The background in events with OS lepton pairs consists primarily of Z/γ^*+jets and W+jets events, while $V\gamma^*$+jets, $\text{t}\bar{\text{t}}$, single
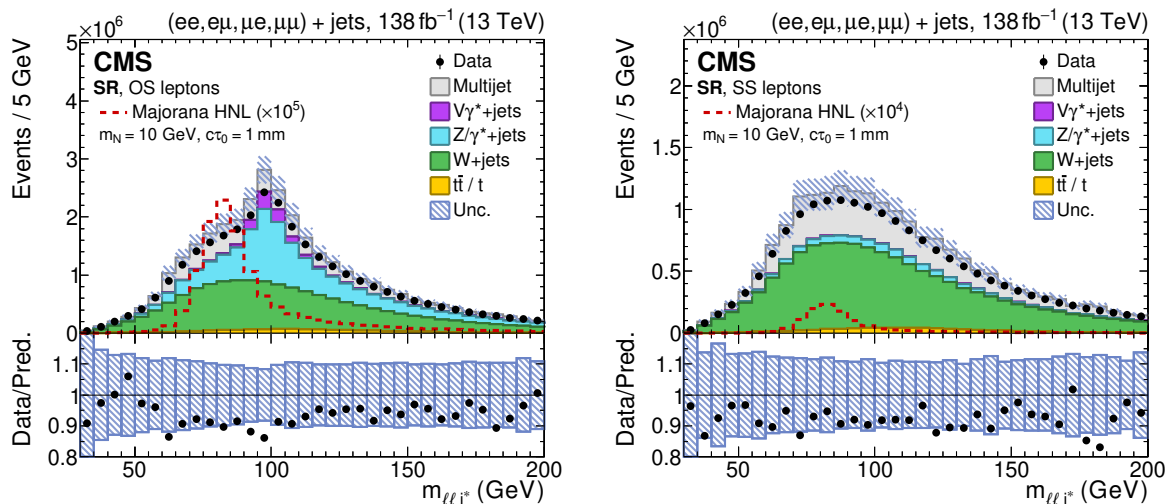
Figure 2. Distributions of $m_{\ell\ell j^\star}$ for events with (left) OS leptons and (right) SS leptons in the signal region. A representative signal scenario for Majorana HNL production with equal coupling to all lepton generations is overlaid with its expected cross section scaled up as indicated in parentheses. The hatched band shows the total experimental systematic uncertainty in the simulated background prediction including the uncertainty from the finite sample size. The bottom panel shows the ratio of data over the prediction.

top quark, and multijet processes are subdominant. A peak around the Z boson mass is seen in Z/γ^*+jets events since $m_{\ell\ell j^\star}$ is mainly calculated from the two leptons momenta when the hadronic activity in j* is low. In SS lepton pair events, multijet and W+jets events get selected because of misidentified leptons and compose the majority of the background. The number of multijet events appears to be slightly overestimated by the simulation resulting in an overall mismatch in normalization between data and prediction, which is however found to be covered by uncertainties. For further analysis, only events in the signal-enhanced region, defined by $70 < m_{\ell\ell j^\star} < 90$ GeV, are kept, whereas the sideband region in $m_{\ell\ell j^\star}$ is used to estimate the background contributions from data (section 6). Overall, the total background is of comparable size in both categories and since the Majorana and Dirac HNL production cross sections are identical, a similar sensitivity for both HNL types is expected.

5 Identification of displaced jets

Displaced jets that originate from the HNL decay products are identified using a jet tagger based on a DNN. The tagger is trained using jets originating from HNL decays with a transverse displacement L_{xy} between $100\,\mu$m and 1 m, where the lower threshold corresponds to a factor 2–4 times the position resolution of the PV [61]. The DNN is trained on various features of the selected jets and parameterized with respect to L_{xy}, resulting in an optimized multiclass classifier that can be applied for a large variety of jets and displacements. The network is based on the developments reported in ref. [62], but its setup has been extended in several aspects to account for the specific properties of jets from HNL decays, as detailed in the following.

The DNN architecture consists of approximately 330 000 parameters. The set of input features includes global jet features, as well as specific features for each type of jet constituent. The global jet features are the jet p_T, $|\eta|$, mass, and area; the fraction of energy carried by the constituents within cones of $\Delta R = 0.1, 0.2, 0.3, 0.4$ with respect to the jet axis; the number of constituents carrying 60 or 90% of the jet energy; the charged, electromagnetic, muon, and electron energy fractions; the variables used in the combined secondary vertex b tagging algorithm [63]; the 1-, 2-, and 3-subjettiness variables [64]; and various event shape observables that are calculated from the constituents in the rest frame of the jet to probe its substructure. In total, 47 global jet features are used.

The features per constituent are grouped into blocks according to their type as follows:

- *Charged PF candidates:* these candidates have an associated track and can thus provide information about the potential displacement of the jet within the tracking volume. The features encapsulate various properties of the track, its displacement with respect to the PV, and whether the track is also linked to a secondary vertex or a PF electron or muon. Up to 25 charged PF candidates are considered per jet, which are sorted according to the significance of their displacement in the transverse plane with respect to the PV. In total, 36 features are used per charged PF candidate.

- *Neutral PF candidates:* features from up to 25 neutral constituents are used as input, which are important for identifying jets from HNL decays that occur at the outer edge of the tracking volume, where the track reconstruction efficiency is low. The neutral candidate features include the likelihood that the candidate stems from pileup interactions as calculated by the PUPPI algorithm [65]. The candidates are sorted by either their distance in ΔR to a secondary vertex or by their p_T in cases where no secondary vertex has been reconstructed. In total, 9 features are used per neutral PF candidate.

- *Secondary vertices:* features from up to four secondary vertices, reconstructed with the inclusive secondary vertex finder algorithm [66], that are found within $\Delta R < 0.4$ of the jet axis and use at least one jet constituent in their reconstruction, are provided as input to the DNN as well. They are sorted by the significance of their displacement in the transverse plane with respect to the PV. In total, 14 features are used per secondary vertex.

- *PF electrons/muons:* if a charged PF candidate is linked to a PF electron or muon, features that are specific to their reconstruction are used as additional inputs. For electrons, the properties of the Gaussian-sum-filter track [67] and matching clusters in the ECAL are used. For muons, the features include details of the global track fit and the hit pattern in the muon chambers. Up to two electrons and muons are considered per jet, which are sorted according to the significance of their displacement in the transverse plane with respect to the PV. In total, 78 (37) features are used per electron (muon) candidate.

In the first stage of the DNN, the various jet constituent features are compressed through a series of one-dimensional convolutions with varying filter sizes using a kernel size of one. The last convolutional layer can be seen as a bottleneck that forces the DNN to extract only the most discriminating information from the larger number of input features, which is then passed on to the next stage. The compressed features of each block are flattened

and concatenated with global jet features and L_{xy}, where the latter acts as a parameter of the DNN [68]. The result is then passed through two dense layers with 200 nodes. At this stage, the network splits into one branch to predict the jet class and into another branch to predict the jet domain (i.e. simulation or data), where each branch consists of another series of dense layers. The following jet classes are considered: jets from the hadronization of gluons or quarks; jets from pileup interactions; jets clustered primarily from prompt e, μ, photons, or hadronically decaying τ leptons; displaced jets from the HNL decay with or without displaced e, μ, or hadronically decaying τ leptons.

In general, the intricate modelling of displaced signatures is less well studied compared to prompt ones. Hence, features of displaced jets can possess a different trend in data compared to simulation. The distribution of output discrimination scores from a classifier, trained solely on simulated events, can differ significantly when evaluated on simulation or data. In a previous study, differences of up to 50% have been seen between the selection efficiencies of data and simulation [62]. In this search, a domain adaptation technique is used to mitigate such differences and effectively calibrate the response of the tagger for simulated events. Technically, a layer is inserted into the domain branch that reverses the gradients of the loss function with respect to the DNN parameters in the preceding layers. During the training, this forces the DNN to retain only discriminating features from the inputs that are domain-invariant [69], i.e. features that are well described by the simulation. The loss function is chosen to approximate the earth mover distance [70], which yields well-defined gradients and thus stabilizes the adversarial training. The relative strength of the domain loss is chosen such that a trade-off is achieved between obtaining a discriminant with approximately equal efficiencies in data and simulation while simultaneously retaining high discrimination between the various jet classes.

The class branch is trained using jets from independent samples of simulated events from various processes. The jets are resampled to obtain a balanced set with equal class proportions as a function of the jet p_T and η. Random L_{xy} values are assigned to background jets that are sampled from the distribution of L_{xy} values of true HNL jets [68]. The domain branch is trained on jets from data and simulated background events in the CR, where the latter are weighted according to the expected cross section per process.

The best discrimination against SM jets is found by calculating the ratios for each displaced jet likelihood over the sum of the SM background likelihoods. The ratios are monotonically mapped to the range 0–1 for simplicity. Per displaced jet, the L_{xy} parameter is chosen in the range 10^{-1}–10^3 mm to maximize the resulting score for each class. For true displaced jets, the score will be the largest when L_{xy} matches the displacement of the HNL, whereas it is randomly distributed for SM jets. The resulting scores are used as follows. For resolved events, the score for displaced jets with and without hadronically decaying τ leptons, $P_q(j^\star)$, is evaluated. On the other hand, for boosted events the flavour of ℓ_2 determines whether the score for displaced jets with electrons, $P_e(j^\star)$, or with muons, $P_\mu(j^\star)$, is evaluated instead. Distributions of the resulting scores are shown in figure 3 for resolved and boosted categories in the CR and SR. In general, the prediction from simulation, normalized to the integrated luminosity, describes the data well in all regions, except for a slight overestimation of multijet events as seen before in figure 2. Selections on the resulting displaced-jet tagger

score can reduce the SM backgrounds by several orders in magnitude. For example, a selection of $P(\mathrm{j}^\star) > 0.6$ reduces the background yield by a factor of about $3000\,(800)$ while retaining $10\,(17\%)$ of signal events for boosted (resolved) events considering the signal scenario in figure 3. In the analysis, optimized thresholds on $P_{\mathrm{q},\ell}(\mathrm{j}^\star)$ are applied ranging from 0.2–0.7 depending on the event category to achieve the best sensitivity, as described later in section 8.

6 Estimation of background processes

Various background sources contribute to the SR, with different relative fractions depending on the category. A substantial background contribution originates from Z/γ^*+jets production in events with two genuine OS leptons of same flavour. In events with either SS leptons or OS leptons of different flavour, the dominant source of background events is misidentified leptons, which primarily originate from W+jets, $\mathrm{V}\gamma^*+$jets, and multijet production, whereas events from $\mathrm{t}\bar{\mathrm{t}}$ production are less prominent. For final states containing electrons, "charge-flip" backgrounds, where the charge of one of the electrons is misidentified, are also possible.

Contributions from background processes are determined from data to accurately account for the reconstruction effects, selection efficiencies, and object calibrations of background events in the final event categories. This procedure has the additional advantage that no large samples of background events have to be simulated and subsequently calibrated for modelling the background contribution in the SR.

The yields in data, n_X^α, from three background-enriched sideband regions $\alpha \in \{\mathrm{A}, \mathrm{B}, \mathrm{C}\}$ in each of the 48 categories X per data-taking period are used to determine the background contribution, b_X^{D}, in a signal-enriched region. The regions are defined by selecting events to be either above or below optimized thresholds on the $P_{\mathrm{q},\ell}(\mathrm{j}^\star)$ score or on the $m_{\ell\ell\mathrm{j}^\star}$ observable, which are found to be independent from studies of simulated events. These selections partition the SR into four orthogonal regions as sketched in figure 4.

A so-called matrix ("ABCD") method is used, where the pass-fail ratio of an event passing the threshold on $P_{\mathrm{q},\ell}(\mathrm{j}^\star)$ is measured in $m_{\ell\ell\mathrm{j}^\star}$ sidebands (50–70 GeV or 90–110 GeV) and then applied to the observed yield found within 70–90 GeV. The yields b_X^{D} are determined through a maximum likelihood fit to data using the following model to properly account for non-Gaussian uncertainties in case of small event yields:

$$L\left(r, \vec{b}, \vec{\theta}, \vec{\kappa}\,\middle|\,\vec{n}\right) = \overset{2016,2017,2018}{\underset{i}{\prod}} \; \overset{\text{resolved,boosted}}{\underset{j}{\prod}} \; \overset{\text{subcategory}}{\underset{k}{\prod}} \; \overset{\text{A,B,C}}{\underset{\alpha}{\prod}} \tag{6.1}$$

$$\times\, \mathrm{Poisson}\left(n_{ijk}^\alpha\,\middle|\,b_{ijk}^\alpha + r\,s_{ijk}^\alpha(\vec{\theta})\right) \mathrm{Poisson}\left(n_{ijk}^{\mathrm{D}}\,\middle|\,b_{ijk}^{\mathrm{D}} + r\,s_{ijk}^{\mathrm{D}}(\vec{\theta})\right) p(\vec{\theta}), \quad b_{ijk}^{\mathrm{D}} \equiv \kappa_{ij}\frac{b_{ijk}^{\mathrm{B}}\,b_{ijk}^{\mathrm{C}}}{b_{ijk}^{\mathrm{A}}},$$

where n_{ijk}^α is the number of events observed in region α with i denoting the data-taking period, j denoting the event topology, and k denoting the subcategory $\{\mathrm{ee}, \mathrm{e}\mu, \mu\mathrm{e}, \mu\mu\} \otimes \{\mathrm{OS}, \mathrm{SS}\} \otimes \{d_{\mathrm{xy}}^{\mathrm{sig}}(\ell_2) \text{ bins}\}$. Nuisance parameters $\vec{\theta}$ that control the effects of systematic uncertainties are constrained through prior probability density functions $p(\vec{\theta})$. A possible signal contamination of $r\,s_{ijk}^\alpha$ in the sidebands is explicitly considered, where r modifies the expected signal yields s_{ijk}^α from simulation for the given HNL scenario under consideration.
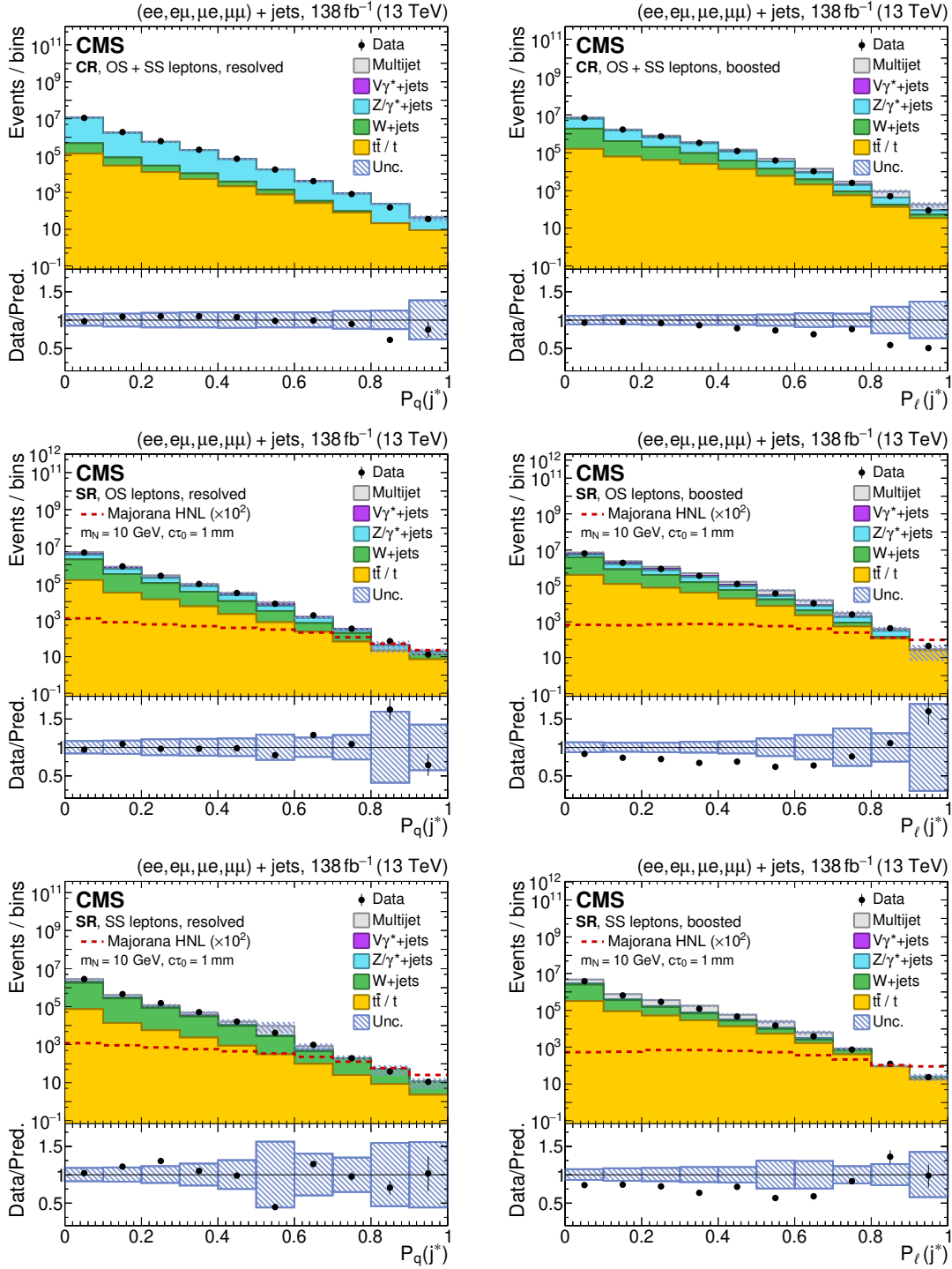
Figure 3. Distributions of the displaced jet tagging score for (left) resolved and (right) boosted categories: (upper row) control region; (middle row) signal region with OS leptons; (lower row) signal region with SS leptons. A representative signal scenario for Majorana HNL production with equal coupling to all lepton generations is overlaid with its expected cross section scaled up as indicated in parentheses. The hatched band shows the total experimental systematic uncertainty in the simulated background prediction including the uncertainty from the finite sample size. The bottom panel shows the ratio of data over the prediction.
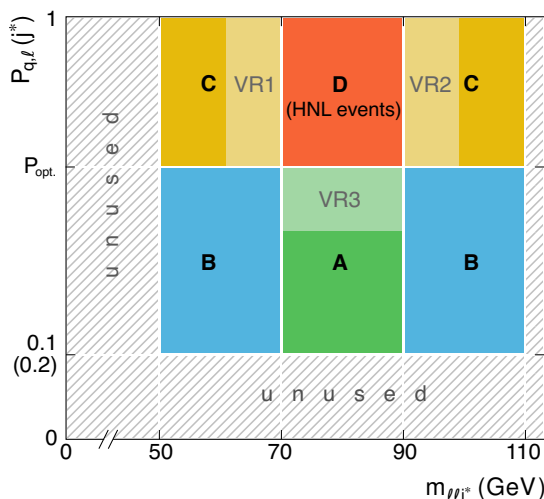
Figure 4. Schematic of the orthogonal regions in the $(m_{\ell\ell \mathrm{j}^\star}, P_{\mathrm{q},\ell}(\mathrm{j}^\star))$ plane, that are used to determine the background in region D from data through an ABCD method. The threshold $P_{\mathrm{opt.}}$ depends on the category. Regions with $P_{\mathrm{q},\ell}(\mathrm{j}^\star) < 0.1\,(0.2)$ for resolved (boosted) events are not considered. The three VRs that are subsets of regions A and C are indicated in lighter shades. The figure is not to scale.

In addition to the signal strength r, fit parameters κ_{ij} are introduced, for which the fitted values will be found to diverge from unity in the presence of a bias from the ABCD method. Separate κ_{ij} parameters are used per data-taking period and per event topology. In summary, the parameters of this fit are r, b_{ijk}^α, $\vec{\theta}$, and κ_{ij}.

The validity of the background estimation method is tested by predicting the data yields in three background-dominated validation regions (VRs) that are defined as follows. The first two VRs comprise events within $m_{\ell\ell \mathrm{j}^\star}$ ranges of 65–70 GeV or 90–100 GeV together with selections on the $P_{\mathrm{q},\ell}(\mathrm{j}^\star)$ scores. For the third VR, events within a $m_{\ell\ell \mathrm{j}^\star}$ range of 70–90 GeV that are within an interval in the $P_{\mathrm{q},\ell}(\mathrm{j}^\star)$ scores below $P_{\mathrm{opt.}}$ are used. The three VRs in the $(m_{\ell\ell \mathrm{j}^\star}, P_{\mathrm{q},\ell}(\mathrm{j}^\star))$ plane are sketched in figure 4. Another test is performed in an additional VR, defined using a narrow $m_{\ell\ell \mathrm{j}^\star}$ window within 5 GeV of region D, comprising subsets of events from both VR1 and VR2, to test the background estimation method close to region D.

Per VR, each κ_{ij} parameter is determined through a simultaneous fit to 24 independent event categories. Overall, the determined event yields agree well with the observations in all VRs and uncertainties of 10–25% are assigned on b_{ijk}^{D}, chosen based on the most significant deviations of κ_{ij} from unity. These uncertainties are implemented in fits of the SR through log-normal priors on the κ_{ij} parameters.

7 Systematic uncertainties

The expected numbers of signal and background events can be affected by several sources of systematic uncertainties. Their impact is modelled through nuisance parameters that change the expected events yields and are correlated across all categories and years, where applicable. Most uncertainties only impact the signal prediction since it is obtained from

simulation, whereas the number of expected background events is determined from data in sideband regions, as detailed in section 6.

A set of systematic uncertainties related to the selection efficiencies and calibration of leptons, jets, and p_T^{miss} is evaluated for simulated events as described below. These are propagated through the displaced jet tagger by recalculating the scores on the modified inputs where applicable.

Systematic uncertainties in the prompt lepton reconstruction, identification, and trigger efficiencies are accounted for by varying p_T and η-dependent normalization factors, derived from data-to-simulation ratios, within their uncertainties. Systematic uncertainties in the identification efficiency of the displaced lepton candidates are taken into account by varying additional scale factors within their uncertainties. These have been derived in $J/\psi \to \mu\mu$ events and in asymmetric $\gamma \to ee$ conversion events. Furthermore, an uncertainty in the lepton track reconstruction efficiency is considered, derived from tracks in $t\bar{t}$-enriched events.

The jet energy scale in simulated events is modified for all jets using the uncertainty associated with the p_T and η-dependent scale factors. The resulting differences are propagated to p_T^{miss}. The jet energy resolution is modified in simulated events by either increasing or decreasing the difference in p_T with respect to the matched jet at the generator level. Random smearing is used when no generator-level jet is found within $\Delta R < 0.4$. The component of p_T^{miss} that is not clustered inside jets, and thus remains uncorrected by the jet energy scale, is varied within its uncertainty.

An uncertainty of 5% in the total inelastic cross section [71] is used when calculating the expected distribution of the number of pileup interactions in data.

An uncertainty in the displaced track reconstruction and jet tagging efficiency, which accounts for differences between data and simulation, is determined using tracks matched to secondary vertices in events from a $t\bar{t}$-enriched region. These differences are parameterized as a function of the track $|d_{xy}|$. A correction and the corresponding uncertainty in the displaced jet tagging efficiency is derived by varying the efficiency of the three most significantly displaced tracks within $j^\star$. These are found to be less than 10% for jets with prompt-like tracks ($d_{xy} < 0.1\,cm$) and in the range 10–20% at larger displacements. Uncertainties in the mistagging efficiency for jets from SM backgrounds are accounted for through the uncertainties in the background estimation.

The factorization and renormalization scales are varied by factors of 2 and 0.5 in simulated signal samples using precomputed weights by the event generator [72]. Only residual changes after the selection are taken as uncertainties while the overall effect on the normalization is considered part of the theoretical uncertainty instead. Uncertainties due to the PDF choice are determined by reweighting each event according to the prescribed variations of the corresponding PDF set.

The integrated luminosities of the 2016, 2017, and 2018 data-taking periods are individually known with uncertainties in the 1.2–2.5% range [73–75], while the total 2016–2018 integrated luminosity has an uncertainty of 1.6%, the improvement in precision reflecting the (uncorrelated) time evolution of some systematic effects.

Uncertainties resulting from the finite size of the simulated samples are incorporated into the likelihood model using the Barlow-Beeston method [76].
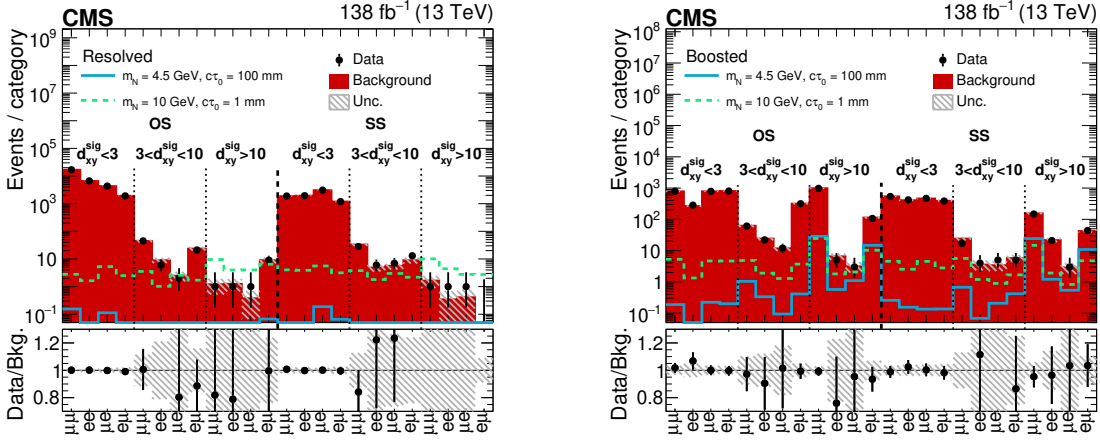
Figure 5. Observed number of events and predicted number of background events per category for (left) resolved and (right) boosted categories. The bin label denotes the flavour of the prompt (ℓ_1) and displaced (ℓ_2) lepton as $\ell_1\ell_2$. Two representative signal scenarios for Majorana HNL production with equal coupling to all lepton generations are overlaid. The lower panels show the ratio of the data to the predicted background. The hatched band shows the total systematic uncertainty in the predicted background.

The background yields are determined in-situ using the likelihood model defined in eq. (6.1), which properly accounts for the statistical uncertainties in the data yields in the sidebands. Additional uncertainties in the range of 10–25% in the background yield are considered to account for the difference in the background estimation per data-taking period and for additional differences between resolved and boosted categories.

In summary, the statistical uncertainties from the sideband regions in the background yields are found to have the largest impact on the determined signal yield for the signal+background hypothesis, which can be as large as 10% depending on the category. Smaller impacts originate from the loose muon reconstruction (7%), the jet tagging efficiency (6%), the loose electron reconstruction (4%), and the jet energy scale and resolution (2%).

8 Results

The thresholds on the $P_{q,\ell}(j^\star)$ scores are optimized per category to yield the best discovery sensitivity [77] to the various HNL scenarios as follows. The expected yields and uncertainties from background processes are determined from data in sideband regions and the expected signal yields are taken from simulation, such that no bias with respect to the observed data can occur. The optimal thresholds are found to be within the range 0.2–0.7, depending on the event category. The resulting background yields are compared to the observed number of events in figure 5. The events in data are found to agree well with the estimated number of background events in each category.

Upper limits on the HNL production cross sections at 95% confidence level (CL) are determined as functions of m_N and the absolute values of the couplings strengths squared $|V_{eN}|^2$, $|V_{\mu N}|^2$, and $|V_{\tau N}|^2$. A modified frequentist approach is employed, which uses the profile likelihood ratio as the test statistic [78], the CL$_s$ criterion [79, 80], and the asymptotic

formulae [81] to approximate the distributions of the test statistic under the background-only and signal-plus-background hypotheses.

Two-dimensional exclusion limits on Dirac and Majorana HNL production are shown in figures 6, 7, and 8 for scenarios of pure coupling, of mixed coupling, and of democratic couplings to all lepton generations, respectively. A broad parameter space in mass and coupling values is excluded by this search. For $m_N \lesssim 8\,\text{GeV}$, most exclusion limits roughly follow a constant $c\tau_0$ value. At higher masses, the cross section becomes too low and, at the same time, sensitivity to displaced scenarios is lost causing the limit curve to turn. At $m_N \gtrsim 14\,\text{GeV}$, the limits have transitioned into a prompt regime and follow a constant cross section value with negligible dependence on m_N for $m_{\ell,q} \ll m_N \ll m_W$. The sensitivity rapidly deteriorates towards the pure τ lepton coupling scenario since $\tau\tau$+jets events are only selected in the analysis in the case of leptonic τ decays to e or μ, whereas τ lepton decays to hadrons are not considered. No limits can be derived for scenarios with $m_N \lesssim 3\,\text{GeV}$ that are close to the pure τ lepton coupling case, because of the tau mass. For some HNL scenarios, the results are compared to an orthogonal search exploiting $N \to \ell^\pm \ell^\mp \nu$ decays, where the two leptons form a displaced vertex [28], which prevents sensitivity to prompt scenarios, resulting in a different trend in the limits at high masses. In this search, the sensitivity to prompt scenarios is achieved by the displaced jet tagger, in part due to the absence of any requirement on the presence (or otherwise) of reconstructed secondary vertices. The best limits are obtained for pure muon coupling scenarios due to the excellent muon identification performance. Coupling strength values as low as $|V_{\mu N}|^2 > 5\,(4) \times 10^{-7}$ are excluded for Dirac (Majorana) HNLs with $m_N = 10\,\text{GeV}$ at 95% CL that correspond to proper decay lengths of $17\,(10)\,\text{mm}$.

Limits on the HNL mass and proper lifetime are presented in figures 9 and 10, respectively, as functions of the relative coupling strengths to the three lepton generations, defined as $f_\ell = |V_{\ell N}|^2 / (|V_{eN}|^2 + |V_{\mu N}|^2 + |V_{\tau N}|^2)$. The results are obtained by interpolating the logarithmic value of the limits linearly between neighbouring points in f_ℓ-space. The most stringent limits are found for pure muon coupling scenarios.

The results obtained from the hadronic HNL decay show a comparable sensitivity as previous HNL searches targeting the orthogonal leptonic final state by the ATLAS, CMS and LHCb Collaborations [20, 21, 25, 26, 28, 31, 32]. In particular, the presented results for the pure electron coupling scenario are found to be more stringent for $m_N \lesssim 4\,\text{GeV}$. These are the first results reported that involve a prompt or long-lived Majorana or Dirac HNL that couples to all three lepton generations in the 2–20 GeV mass range.

9 Summary

A search is presented for long-lived heavy neutral leptons (HNLs), which are predicted in extensions of the standard model of particle physics through a seesaw mechanism. Dirac or Majorana HNLs can mix with the three standard model lepton generations in a nontrivial way, resulting in lepton flavour number violation. Hence, a complete set of coupling scenarios involving all three lepton generations is considered. A novelty of this analysis is the simultaneous sensitivity to prompt and displaced scenarios through the use of a dedicated displaced jet tagger that does not explicitly rely on the presence of secondary vertices.
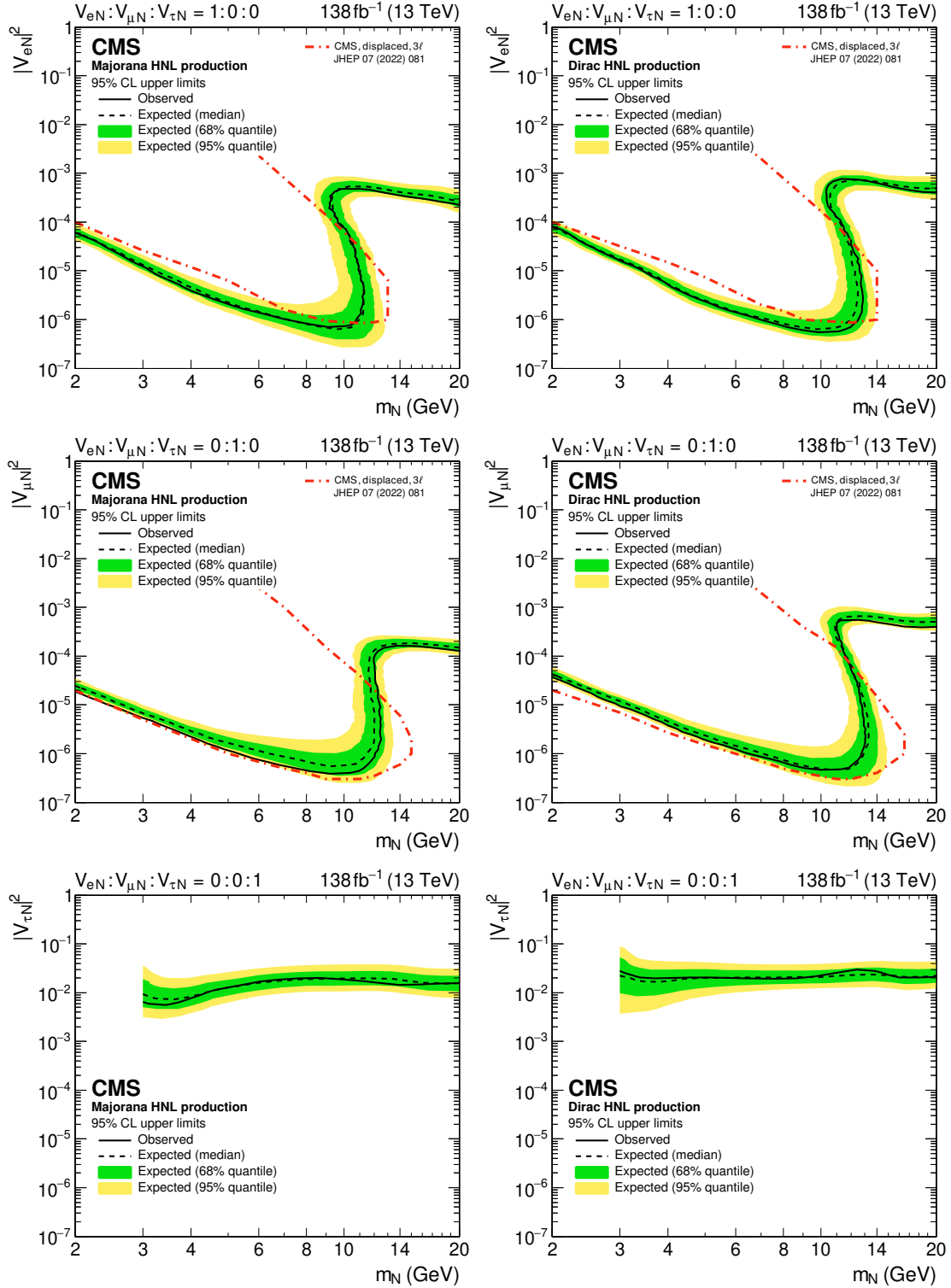
Figure 6. Expected and observed 95% CL limits on (left) Majorana and (right) Dirac HNL production as functions of the HNL mass and coupling strengths for (upper row) pure electron, (middle row) pure muon, and (lower row) pure τ lepton coupling scenarios. For the last coupling case no limits are derived for $m_N \lesssim 3\,\text{GeV}$ because of the tau mass. The dashed-dotted line shows the result of an orthogonal CMS analysis targeting HNL decays to leptons.
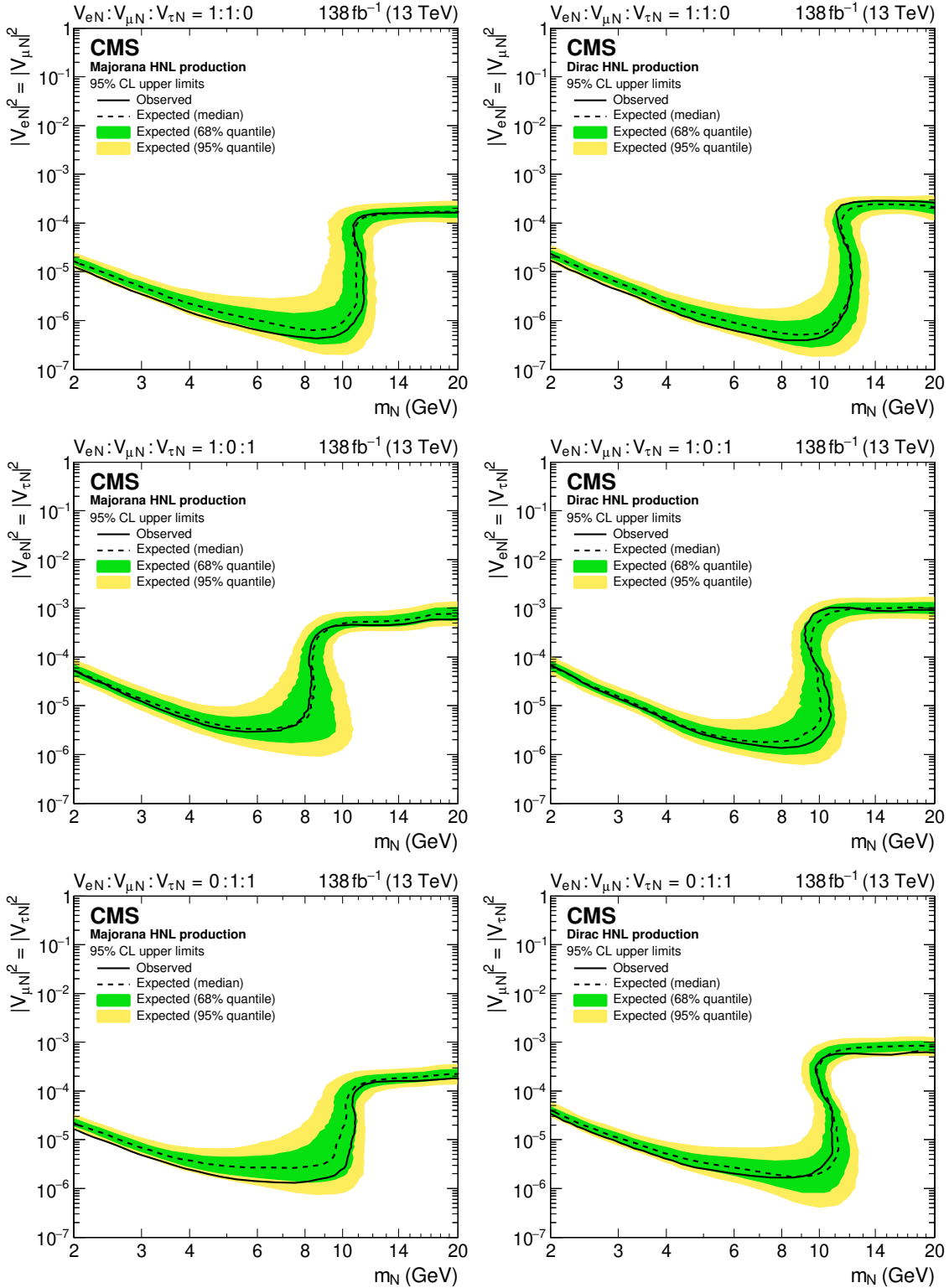
Figure 7. Expected and observed 95% CL limits on (left) Majorana and (right) Dirac HNL production for various coupling scenarios as functions of the HNL mass and coupling strengths: (upper row) mixed e-μ couplings; (middle row) mixed e-τ couplings; (lower row) mixed μ-τ couplings. The relative ratios of the coupling per lepton generation are indicated in the plots.
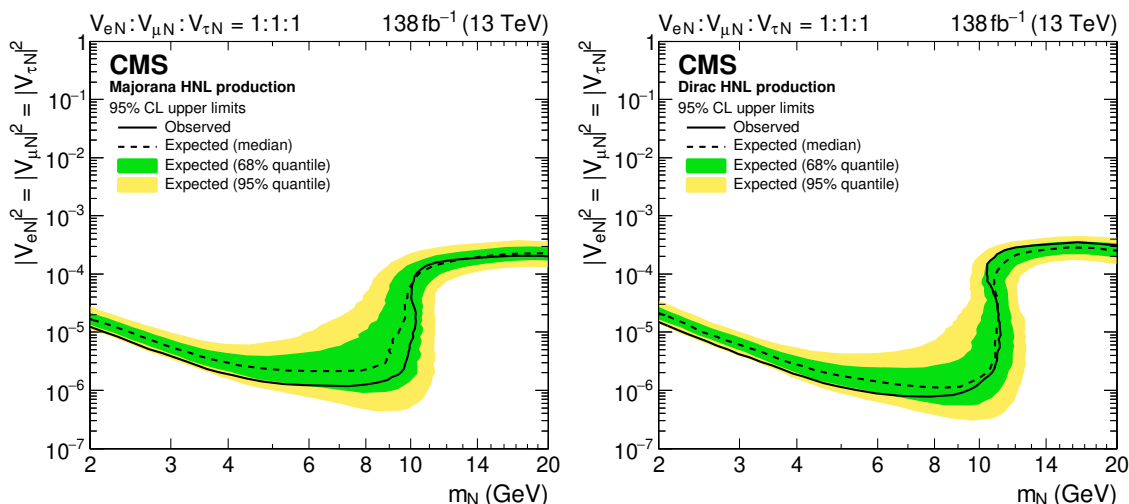
Figure 8. Expected and observed 95% CL limits on (left) Majorana and (right) Dirac HNL production for the democratic couplings to all lepton generation scenario as functions of the HNL mass and coupling strengths.

A data sample of proton-proton collision events recorded with the CMS experiment at the CERN LHC at a centre-of-mass energy of 13 TeV is analyzed, corresponding to an integrated luminosity of $138\,\mathrm{fb}^{-1}$. Events containing two leptons (electrons or muons) and jets are selected and categorized according to the lepton flavour and electrical charge, the displacement of the lower-momentum lepton, and whether the lepton overlaps with a nearby jet. Jets originating from the decay of a long-lived HNL are identified through a deep neural network using various features of the jet and its constituent particles. The network training relies on simulated event samples that cover a broad range of HNL masses and lifetimes, and acts as a powerful discriminant for jets that are spatially separated from the luminous region, even in the absence of reconstructed secondary vertices.

Contributions from background processes are determined from data in sideband regions. No excess of events in the data over the expected background is observed. Upper limits on the HNL production cross section are determined as functions of the HNL mass and the three coupling strengths to each lepton generation. Exclusion limits are presented in the coupling-mass plane, as lower limits on the HNL lifetime, and on the HNL mass. Results are provided for Dirac and Majorana HNL production considering various coupling combinations. The most stringent limit on the coupling strength is obtained for pure muon coupling scenarios, with values of $|V_{\mu N}|^2 > 5\,(4) \times 10^{-7}$ excluded for Dirac (Majorana) HNLs with a mass of 10 GeV at a confidence level of 95% that correspond to proper decay lengths of 17 (10) mm.

This analysis is the first HNL search at the LHC that targets long-lived and hadronically decaying HNLs in the 2–20 GeV mass range, with inclusive coupling to all three lepton generations. The results show comparable sensitivity to an orthogonal analysis that targets long-lived HNLs decaying to leptons.
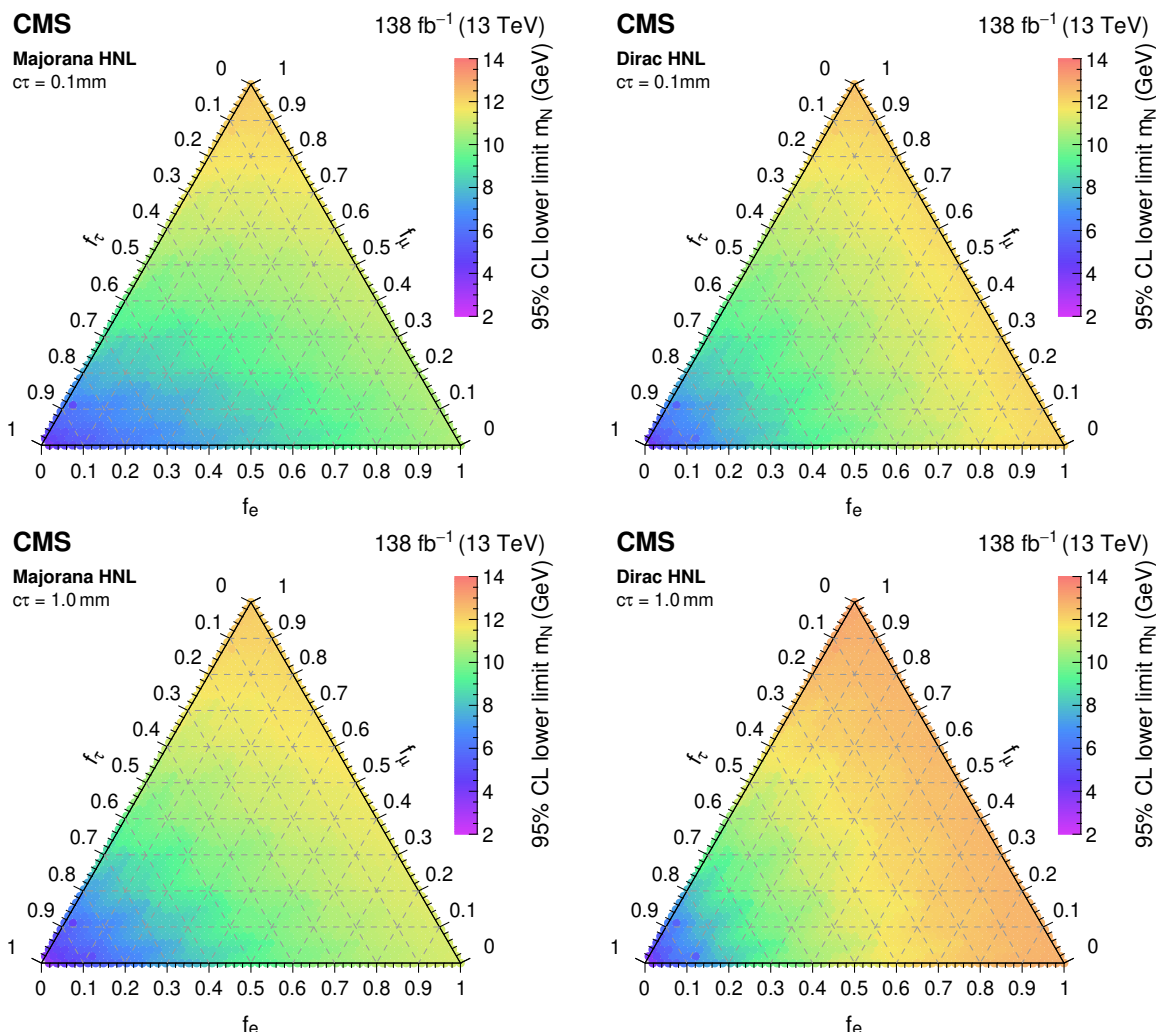
Figure 9. Observed 95% CL lower limits on the (left column) Majorana and (right column) Dirac HNL mass as functions of the relative couplings to the three lepton generations considering a fixed proper decay length of (upper row) 0.1 mm and (lower row) 1 mm. The limits are determined for $m_\mathrm{N} > 3\,\mathrm{GeV}$.

Acknowledgments

Figure 10. Observed 95% CL lower limits on the (left column) Majorana and (right column) Dirac HNL proper decay length as functions of the relative couplings to the three lepton generations considering a fixed mass of (upper row) 4.5 GeV and (lower row) 8.0 GeV.

References

[1] SUPER-KAMIOKANDE collaboration, *Evidence for oscillation of atmospheric neutrinos*, *[Phys. Rev. Lett.](#)* **81** (1998) 1562 [[hep-ex/9807003](#)] [[INSPIRE](#)].

[2] SNO collaboration, *Direct evidence for neutrino flavor transformation from neutral current interactions in the Sudbury Neutrino Observatory*, *[Phys. Rev. Lett.](#)* **89** (2002) 011301 [[nucl-ex/0204008](#)] [[INSPIRE](#)].

[3] I. Esteban et al., *Global analysis of three-flavour neutrino oscillations: synergies and tensions in the determination of θ_{23}, δ_{CP}, and the mass ordering*, *[JHEP](#)* **01** (2019) 106 [[arXiv:1811.05487](#)] [[INSPIRE](#)].

[4] KATRIN collaboration, *Direct neutrino-mass measurement with sub-electronvolt sensitivity*, *Nature Phys.* **18** (2022) 160 [`arXiv:2105.08533`] [inSPIRE].

[5] PARTICLE DATA GROUP collaboration, *Review of particle physics*, *PTEP* **2022** (2022) 083C01 [inSPIRE].

[6] P. Minkowski, $\mu \to e\gamma$ *at a rate of one out of* 10^9 *muon decays?*, *Phys. Lett. B* **67** (1977) 421 [inSPIRE].

[7] M. Gell-Mann, P. Ramond and R. Slansky, *Complex spinors and unified theories*, *Conf. Proc. C* **790927** (1979) 315 [`arXiv:1306.4669`] [inSPIRE].

[8] T. Yanagida, *Horizontal gauge symmetry and masses of neutrinos*, in the proceedings of the *Seesaw* 25, (2005) [`DOI:10.1142/9789812702210_0019`].

[9] R.N. Mohapatra and G. Senjanovic, *Neutrino mass and spontaneous parity nonconservation*, *Phys. Rev. Lett.* **44** (1980) 912 [inSPIRE].

[10] J. Schechter and J.W.F. Valle, *Neutrino masses in* SU(2) × U(1) *theories*, *Phys. Rev. D* **22** (1980) 2227 [inSPIRE].

[11] R. Foot, H. Lew, X.G. He and G.C. Joshi, *Seesaw neutrino masses induced by a triplet of leptons*, *Z. Phys. C* **44** (1989) 441 [inSPIRE].

[12] K. Bondarenko, A. Boyarsky, D. Gorbunov and O. Ruchayskiy, *Phenomenology of GeV-scale heavy neutral leptons*, *JHEP* **11** (2018) 032 [`arXiv:1805.08567`] [inSPIRE].

[13] T. Asaka and M. Shaposhnikov, *The νMSM, dark matter and baryon asymmetry of the universe*, *Phys. Lett. B* **620** (2005) 17 [`hep-ph/0505013`] [inSPIRE].

[14] T. Asaka, S. Blanchet and M. Shaposhnikov, *The νMSM, dark matter and neutrino masses*, *Phys. Lett. B* **631** (2005) 151 [`hep-ph/0503065`] [inSPIRE].

[15] A. Boyarsky, O. Ruchayskiy and M. Shaposhnikov, *The role of sterile neutrinos in cosmology and astrophysics*, *Ann. Rev. Nucl. Part. Sci.* **59** (2009) 191 [`arXiv:0901.0011`] [inSPIRE].

[16] M. Drewes, *The phenomenology of right handed neutrinos*, *Int. J. Mod. Phys. E* **22** (2013) 1330019 [`arXiv:1303.6912`] [inSPIRE].

[17] F.F. Deppisch, P.S. Bhupal Dev and A. Pilaftsis, *Neutrinos and collider physics*, *New J. Phys.* **17** (2015) 075019 [`arXiv:1502.06541`] [inSPIRE].

[18] J. Beacham et al., *Physics beyond colliders at CERN: beyond the Standard Model working group report*, *J. Phys. G* **47** (2020) 010501 [`arXiv:1901.09966`] [inSPIRE].

[19] ATLAS collaboration, *Search for a right-handed gauge boson decaying into a high-momentum heavy neutrino and a charged lepton in pp collisions with the ATLAS detector at* $\sqrt{s} = 13$ *TeV*, *Phys. Lett. B* **798** (2019) 134942 [`arXiv:1904.12679`] [inSPIRE].

[20] ATLAS collaboration, *Search for heavy neutral leptons in decays of W bosons produced in* 13 *TeV pp collisions using prompt and displaced signatures with the ATLAS detector*, *JHEP* **10** (2019) 265 [`arXiv:1905.09787`] [inSPIRE].

[21] ATLAS collaboration, *Search for heavy neutral leptons in decays of W bosons using a dilepton displaced vertex in* $\sqrt{s} = 13$ *TeV pp collisions with the ATLAS detector*, *Phys. Rev. Lett.* **131** (2023) 061803 [`arXiv:2204.11988`] [inSPIRE].

[22] ATLAS collaboration, *Search for Majorana neutrinos in same-sign WW scattering events from pp collisions at* $\sqrt{s} = 13$ *TeV*, *Eur. Phys. J. C* **83** (2023) 824 [`arXiv:2305.14931`] [inSPIRE].

[23] ATLAS collaboration, *Search for heavy Majorana or Dirac neutrinos and right-handed W gauge bosons in final states with charged leptons and jets in pp collisions at* $\sqrt{s} = 13$ *TeV with the ATLAS detector*, *Eur. Phys. J. C* **83** (2023) 1164 [`arXiv:2304.09553`] [inSPIRE].

[24] CMS collaboration, *Search for a heavy right-handed W boson and a heavy neutrino in events with two same-flavor leptons and two jets at $\sqrt{s} = 13$ TeV*, *JHEP* **05** (2018) 148 [arXiv:1803.11116] [InSPIRE].

[25] CMS collaboration, *Search for heavy neutral leptons in events with three charged leptons in proton-proton collisions at $\sqrt{s} = 13$ TeV*, *Phys. Rev. Lett.* **120** (2018) 221801 [arXiv:1802.02965] [InSPIRE].

[26] CMS collaboration, *Search for heavy Majorana neutrinos in same-sign dilepton channels in proton-proton collisions at $\sqrt{s} = 13$ TeV*, *JHEP* **01** (2019) 122 [arXiv:1806.10905] [InSPIRE].

[27] CMS collaboration, *Search for heavy neutrinos and third-generation leptoquarks in hadronic states of two τ leptons and two jets in proton-proton collisions at $\sqrt{s} = 13$ TeV*, *JHEP* **03** (2019) 170 [arXiv:1811.00806] [InSPIRE].

[28] CMS collaboration, *Search for long-lived heavy neutral leptons with displaced vertices in proton-proton collisions at $\sqrt{s} = 13$ TeV*, *JHEP* **07** (2022) 081 [arXiv:2201.05578] [InSPIRE].

[29] CMS collaboration, *Probing heavy Majorana neutrinos and the Weinberg operator through vector boson fusion processes in proton-proton collisions at $\sqrt{s} = 13$ TeV*, *Phys. Rev. Lett.* **131** (2023) 011803 [arXiv:2206.08956] [InSPIRE].

[30] CMS collaboration, *Search for a heavy composite Majorana neutrino in events with dilepton signatures from proton-proton collisions at $\sqrt{s} = 13$ TeV*, *Phys. Lett. B* **843** (2023) 137803 [arXiv:2210.03082] [InSPIRE].

[31] LHCb collaboration, *Search for heavy neutral leptons in $W^{+} \to \mu^{+}\mu^{\pm}$jet decays*, *Eur. Phys. J. C* **81** (2021) 248 [arXiv:2011.05263] [InSPIRE].

[32] LHCb collaboration, *Search for long-lived particles decaying to $e^{\pm}\mu^{\mp}\nu$*, *Eur. Phys. J. C* **81** (2021) 261 [arXiv:2012.02696] [InSPIRE].

[33] M. Chrzaszcz et al., *A frequentist analysis of three right-handed neutrinos with GAMBIT*, *Eur. Phys. J. C* **80** (2020) 569 [arXiv:1908.02302] [InSPIRE].

[34] *HEPData record for this analysis*, CMS-EXO-21-013, (2023).

[35] CMS collaboration, *The CMS experiment at the CERN LHC*, 2008 *JINST* **3** S08004 [InSPIRE].

[36] CMS collaboration, *Particle-flow reconstruction and global event description with the CMS detector*, 2017 *JINST* **12** P10003 [arXiv:1706.04965] [InSPIRE].

[37] M. Cacciari, G.P. Salam and G. Soyez, *The anti-k_t jet clustering algorithm*, *JHEP* **04** (2008) 063 [arXiv:0802.1189] [InSPIRE].

[38] CMS collaboration, *Technical proposal for the phase-II upgrade of the CMS detector*, CERN-LHCC-2015-010, CERN, Geneva, Switzerland (2015) [DOI:10.17181/CERN.VU8I.D59J].

[39] CMS collaboration, *Performance of missing transverse momentum reconstruction in proton-proton collisions at $\sqrt{s} = 13$ TeV using the CMS detector*, 2019 *JINST* **14** P07004 [arXiv:1903.06078] [InSPIRE].

[40] CMS collaboration, *Performance of the CMS level-1 trigger in proton-proton collisions at $\sqrt{s} = 13$ TeV*, 2020 *JINST* **15** P10017 [arXiv:2006.10165] [InSPIRE].

[41] CMS collaboration, *The CMS trigger system*, 2017 *JINST* **12** P01020 [arXiv:1609.02366] [InSPIRE].

[42] CMS collaboration, *Electron and photon reconstruction and identification with the CMS experiment at the CERN LHC*, 2021 *JINST* **16** P05014 [arXiv:2012.06888] [InSPIRE].

[43] CMS collaboration, *Performance of the CMS muon trigger system in proton-proton collisions at* $\sqrt{s} = 13$ *TeV*, 2021 *JINST* **16** P07001 [arXiv:2102.04790] [INSPIRE].

[44] J. Alwall et al., *The automated computation of tree-level and next-to-leading order differential cross sections, and their matching to parton shower simulations*, *JHEP* **07** (2014) 079 [arXiv:1405.0301] [INSPIRE].

[45] NNPDF collaboration, *Parton distributions from high-precision collider data*, *Eur. Phys. J. C* **77** (2017) 663 [arXiv:1706.00428] [INSPIRE].

[46] T. Sjöstrand et al., *An introduction to PYTHIA* 8.2, *Comput. Phys. Commun.* **191** (2015) 159 [arXiv:1410.3012] [INSPIRE].

[47] CMS collaboration, *Event generator tunes obtained from underlying event and multiparton scattering measurements*, *Eur. Phys. J. C* **76** (2016) 155 [arXiv:1512.00815] [INSPIRE].

[48] CMS collaboration, *Extraction and validation of a new set of CMS PYTHIA8 tunes from underlying-event measurements*, *Eur. Phys. J. C* **80** (2020) 4 [arXiv:1903.12179] [INSPIRE].

[49] O. Mattelaer, *On the maximal use of Monte Carlo samples: re-weighting events at NLO accuracy*, *Eur. Phys. J. C* **76** (2016) 674 [arXiv:1607.00763] [INSPIRE].

[50] A. Ali, E. Pietarinen, G. Kramer and J. Willrodt, *A QCD analysis of the high-energy e^+e^- data from PETRA*, *Phys. Lett. B* **93** (1980) 155 [INSPIRE].

[51] A. Atre, T. Han, S. Pascoli and B. Zhang, *The search for heavy Majorana neutrinos*, *JHEP* **05** (2009) 030 [arXiv:0901.3589] [INSPIRE].

[52] D. Alva, T. Han and R. Ruiz, *Heavy Majorana neutrinos from $W\gamma$ fusion at hadron colliders*, *JHEP* **02** (2015) 072 [arXiv:1411.7305] [INSPIRE].

[53] C. Degrande, O. Mattelaer, R. Ruiz and J. Turner, *Fully-automated precision predictions for heavy neutrino production mechanisms at hadron colliders*, *Phys. Rev. D* **94** (2016) 053002 [arXiv:1602.06957] [INSPIRE].

[54] S. Pascoli, R. Ruiz and C. Weiland, *Heavy neutrinos with dynamic jet vetoes: multilepton searches at $\sqrt{s} = 14$, 27, and 100 TeV*, *JHEP* **06** (2019) 049 [arXiv:1812.08750] [INSPIRE].

[55] S. Frixione, P. Nason and G. Ridolfi, *A positive-weight next-to-leading-order Monte Carlo for heavy flavour hadroproduction*, *JHEP* **09** (2007) 126 [arXiv:0707.3088] [INSPIRE].

[56] S. Alioli, P. Nason, C. Oleari and E. Re, *A general framework for implementing NLO calculations in shower Monte Carlo programs: the POWHEG BOX*, *JHEP* **06** (2010) 043 [arXiv:1002.2581] [INSPIRE].

[57] R. Frederix, E. Re and P. Torrielli, *Single-top t-channel hadroproduction in the four-flavour scheme with POWHEG and aMC@NLO*, *JHEP* **09** (2012) 130 [arXiv:1207.5391] [INSPIRE].

[58] GEANT4 collaboration, *GEANT4 — a simulation toolkit*, *Nucl. Instrum. Meth. A* **506** (2003) 250 [INSPIRE].

[59] CMS collaboration, *Performance of the CMS muon detector and muon reconstruction with proton-proton collisions at $\sqrt{s} = 13$ TeV*, 2018 *JINST* **13** P06015 [arXiv:1804.04528] [INSPIRE].

[60] CMS collaboration, *Jet energy scale and resolution in the CMS experiment in pp collisions at 8 TeV*, 2017 *JINST* **12** P02014 [arXiv:1607.03663] [INSPIRE].

[61] CMS collaboration, *Description and performance of track and primary-vertex reconstruction with the CMS tracker*, 2014 *JINST* **9** P10009 [arXiv:1405.6569] [INSPIRE].

[62] CMS collaboration, *A deep neural network to search for new long-lived particles decaying to jets*, *Mach. Learn. Sci. Tech.* **1** (2020) 035012 [arXiv:1912.12238] [INSPIRE].

[63] CMS collaboration, *Identification of heavy-flavour jets with the CMS detector in pp collisions at 13 TeV*, 2018 *JINST* **13** P05011 [arXiv:1712.07158] [INSPIRE].

[64] J. Thaler and K. Van Tilburg, *Identifying boosted objects with N-subjettiness*, *JHEP* **03** (2011) 015 [arXiv:1011.2268] [INSPIRE].

[65] D. Bertolini, P. Harris, M. Low and N. Tran, *Pileup per particle identification*, *JHEP* **10** (2014) 059 [arXiv:1407.6013] [INSPIRE].

[66] CMS collaboration, *Measurement of $B\bar{B}$ angular correlations based on secondary vertex reconstruction at $\sqrt{s} = 7$ TeV*, *JHEP* **03** (2011) 136 [arXiv:1102.3194] [INSPIRE].

[67] W. Adam, R. Fruhwirth, A. Strandlie and T. Todorov, *Reconstruction of electrons with the Gaussian sum filter in the CMS tracker at LHC*, *eConf C* **0303241** (2003) TULT009 [physics/0306087] [INSPIRE].

[68] P. Baldi et al., *Parameterized neural networks for high-energy physics*, *Eur. Phys. J. C* **76** (2016) 235 [arXiv:1601.07913] [INSPIRE].

[69] Y. Ganin and V. Lempitsky, *Unsupervised domain adaptation by backpropagation*, arXiv:1409.7495 [INSPIRE].

[70] M. Arjovsky, S. Chintala and L. Bottou, *Wasserstein GAN*, arXiv:1701.07875 [INSPIRE].

[71] CMS collaboration, *Measurement of the inelastic proton-proton cross section at $\sqrt{s} = 13$ TeV*, *JHEP* **07** (2018) 161 [arXiv:1802.02613] [INSPIRE].

[72] A. Kalogeropoulos and J. Alwall, *The SysCalc code: a tool to derive theoretical systematic uncertainties*, arXiv:1801.08401 [INSPIRE].

[73] CMS collaboration, *Precision luminosity measurement in proton-proton collisions at $\sqrt{s} = 13$ TeV in 2015 and 2016 at CMS*, *Eur. Phys. J. C* **81** (2021) 800 [arXiv:2104.01927] [INSPIRE].

[74] CMS collaboration, *CMS luminosity measurement for the 2017 data-taking period at $\sqrt{s} = 13$ TeV*, CMS-PAS-LUM-17-004, CERN, Geneva, Switzerland (2018).

[75] CMS collaboration, *CMS luminosity measurement for the 2018 data-taking period at $\sqrt{s} = 13$ TeV*, CMS-PAS-LUM-18-002, CERN, Geneva, Switzerland (2019).

[76] R.J. Barlow and C. Beeston, *Fitting using finite Monte Carlo samples*, *Comput. Phys. Commun.* **77** (1993) 219 [INSPIRE].

[77] G. Cowan, *Discovery sensitivity for a counting experiment with background uncertainty*, technical report, http://www.pp.rhul.ac.uk/~cowan/stat/medsig/medsigNote.pdf (2012).

[78] ATLAS and CMS collaborations and LHC HIGGS combination group, *Procedure for the LHC Higgs boson search combination in Summer 2011*, CMS-NOTE-2011-005, CERN, Geneva, Switzerland (2011).

[79] T. Junk, *Confidence level computation for combining searches with small statistics*, *Nucl. Instrum. Meth. A* **434** (1999) 435 [hep-ex/9902006] [INSPIRE].

[80] A.L. Read, *Presentation of search results: the CL_s technique*, *J. Phys. G* **28** (2002) 2693 [INSPIRE].

[81] G. Cowan, K. Cranmer, E. Gross and O. Vitells, *Asymptotic formulae for likelihood-based tests of new physics*, *Eur. Phys. J. C* **71** (2011) 1554 [*Erratum ibid.* **73** (2013) 2501] [arXiv:1007.1727] [INSPIRE].

The CMS collaboration

Yerevan Physics Institute, Yerevan, Armenia

A. Hayrapetyan, A. Tumasyan [1]

Institut für Hochenergiephysik, Vienna, Austria

W. Adam, J.W. Andrejkovic, T. Bergauer, S. Chatterjee, K. Damanakis, M. Dragicevic, P.S. Hussain, M. Jeitler [2], N. Krammer, A. Li, D. Liko, I. Mikulec, J. Schieck [2], R. Schöfbeck, D. Schwarz, M. Sonawane, S. Templ, W. Waltenberger, C.-E. Wulz [2]

Universiteit Antwerpen, Antwerpen, Belgium

M.R. Darwish [3], T. Janssen, P. Van Mechelen

Vrije Universiteit Brussel, Brussel, Belgium

E.S. Bols, J. D'Hondt, S. Dansana, A. De Moor, M. Delcourt, H. El Faham, S. Lowette, I. Makarenko, D. Müller, A.R. Sahasransu, S. Tavernier, M. Tytgat [4], G.P. Van Onsem, S. Van Putte, D. Vannerom

Université Libre de Bruxelles, Bruxelles, Belgium

B. Clerbaux, A.K. Das, G. De Lentdecker, L. Favart, P. Gianneios, D. Hohov, J. Jaramillo, A. Khalilzadeh, K. Lee, M. Mahdavikhorrami, A. Malara, S. Paredes, L. Pétré, N. Postiau, L. Thomas, M. Vanden Bemden, C. Vander Velde, P. Vanlaer

Ghent University, Ghent, Belgium

M. De Coen, D. Dobur, Y. Hong, J. Knolle, L. Lambrecht, G. Mestdach, K. Mota Amarilo, C. Rendón, A. Samalan, K. Skovpen, N. Van Den Bossche, J. van der Linden, L. Wezenbeek

Université Catholique de Louvain, Louvain-la-Neuve, Belgium

A. Benecke, A. Bethani, G. Bruno, C. Caputo, C. Delaere, I.S. Donertas, A. Giammanco, K. Jaffel, Sa. Jain, V. Lemaitre, J. Lidrych, P. Mastrapasqua, K. Mondal, T.T. Tran, S. Wertz

Centro Brasileiro de Pesquisas Fisicas, Rio de Janeiro, Brazil

G.A. Alves, E. Coelho, C. Hensel, T. Menezes De Oliveira, A. Moraes, P. Rebello Teles, M. Soeiro

Universidade do Estado do Rio de Janeiro, Rio de Janeiro, Brazil

W.L. Aldá Júnior, M. Alves Gallo Pereira, M. Barroso Ferreira Filho, H. Brandao Malbouisson, W. Carvalho, J. Chinellato [5], E.M. Da Costa, G.G. Da Silveira [6], D. De Jesus Damiao, S. Fonseca De Souza, R. Gomes De Souza, J. Martins [7], C. Mora Herrera, L. Mundim, H. Nogima, J.P. Pinheiro, A. Santoro, A. Sznajder, M. Thiel, A. Vilela Pereira

The CMS collaboration

Yerevan Physics Institute, Yerevan, Armenia

A. Hayrapetyan, A. Tumasyan [1]

Institut für Hochenergiephysik, Vienna, Austria

W. Adam, J.W. Andrejkovic, T. Bergauer, S. Chatterjee, K. Damanakis, M. Dragicevic, P.S. Hussain, M. Jeitler [2], N. Krammer, A. Li, D. Liko, I. Mikulec, J. Schieck [2], R. Schöfbeck, D. Schwarz, M. Sonawane, S. Templ, W. Waltenberger, C.-E. Wulz [2]

Universiteit Antwerpen, Antwerpen, Belgium

M.R. Darwish [3], T. Janssen, P. Van Mechelen

Vrije Universiteit Brussel, Brussel, Belgium

E.S. Bols, J. D'Hondt, S. Dansana, A. De Moor, M. Delcourt, H. El Faham, S. Lowette, I. Makarenko, D. Müller, A.R. Sahasransu, S. Tavernier, M. Tytgat [4], G.P. Van Onsem, S. Van Putte, D. Vannerom

Université Libre de Bruxelles, Bruxelles, Belgium

B. Clerbaux, A.K. Das, G. De Lentdecker, L. Favart, P. Gianneios, D. Hohov, J. Jaramillo, A. Khalilzadeh, K. Lee, M. Mahdavikhorrami, A. Malara, S. Paredes, L. Pétré, N. Postiau, L. Thomas, M. Vanden Bemden, C. Vander Velde, P. Vanlaer

Ghent University, Ghent, Belgium

M. De Coen, D. Dobur, Y. Hong, J. Knolle, L. Lambrecht, G. Mestdach, K. Mota Amarilo, C. Rendón, A. Samalan, K. Skovpen, N. Van Den Bossche, J. van der Linden, L. Wezenbeek

Université Catholique de Louvain, Louvain-la-Neuve, Belgium

A. Benecke, A. Bethani, G. Bruno, C. Caputo, C. Delaere, I.S. Donertas, A. Giammanco, K. Jaffel, Sa. Jain, V. Lemaitre, J. Lidrych, P. Mastrapasqua, K. Mondal, T.T. Tran, S. Wertz

Centro Brasileiro de Pesquisas Fisicas, Rio de Janeiro, Brazil

G.A. Alves, E. Coelho, C. Hensel, T. Menezes De Oliveira, A. Moraes, P. Rebello Teles, M. Soeiro

Universidade do Estado do Rio de Janeiro, Rio de Janeiro, Brazil

W.L. Aldá Júnior, M. Alves Gallo Pereira, M. Barroso Ferreira Filho, H. Brandao Malbouisson, W. Carvalho, J. Chinellato [5], E.M. Da Costa, G.G. Da Silveira [6], D. De Jesus Damiao, S. Fonseca De Souza, R. Gomes De Souza, J. Martins [7], C. Mora Herrera, L. Mundim, H. Nogima, J.P. Pinheiro, A. Santoro, A. Sznajder, M. Thiel, A. Vilela Pereira

Universidade Estadual Paulista, Universidade Federal do ABC, São Paulo, Brazil

C.A. Bernardes [6], L. Calligaris, T.R. Fernandez Perez Tomei, E.M. Gregores,
P.G. Mercadante, S.F. Novaes, B. Orzari, Sandra S. Padula

Institute for Nuclear Research and Nuclear Energy, Bulgarian Academy of Sciences, Sofia, Bulgaria

A. Aleksandrov, G. Antchev, R. Hadjiiska, P. Iaydjiev, M. Misheva, M. Shopova,
G. Sultanov

University of Sofia, Sofia, Bulgaria

A. Dimitrov, L. Litov, B. Pavlov, P. Petkov, A. Petrov, E. Shumka

Instituto De Alta Investigación, Universidad de Tarapacá, Casilla 7 D, Arica, Chile

S. Keshri, S. Thakur

Beihang University, Beijing, China

T. Cheng, T. Javaid, L. Yuan

Department of Physics, Tsinghua University, Beijing, China

Z. Hu, J. Liu, K. Yi [8,9]

Institute of High Energy Physics, Beijing, China

G.M. Chen [10], H.S. Chen [10], M. Chen [10], F. Iemmi, C.H. Jiang, A. Kapoor [11], H. Liao,
Z.-A. Liu [12], R. Sharma [13], J.N. Song [12], J. Tao, C. Wang [10], J. Wang, Z. Wang [10], H. Zhang

State Key Laboratory of Nuclear Physics and Technology, Peking University, Beijing, China

A. Agapitos, Y. Ban, A. Levin, C. Li, Q. Li, Y. Mao, S.J. Qian, X. Sun, D. Wang,
H. Yang, L. Zhang, C. Zhou

Sun Yat-Sen University, Guangzhou, China

Z. You

University of Science and Technology of China, Hefei, China

N. Lu

Nanjing Normal University, Nanjing, China

G. Bauer [14]

Institute of Modern Physics and Key Laboratory of Nuclear Physics and Ion-beam Application (MOE) — Fudan University, Shanghai, China

X. Gao [15], D. Leggat, H. Okawa

Zhejiang University, Hangzhou, Zhejiang, China

Z. Lin, C. Lu, M. Xiao

Universidad de Los Andes, Bogota, Colombia

C. Avila, D.A. Barbosa Trujillo, A. Cabrera, C. Florez, J. Fraga, J.A. Reyes Vega

Universidad de Antioquia, Medellin, Colombia

J. Mejia Guisao, F. Ramirez, M. Rodriguez, J.D. Ruiz Alvarez

University of Split, Faculty of Electrical Engineering, Mechanical Engineering and Naval Architecture, Split, Croatia

D. Giljanovic, N. Godinovic, D. Lelas, A. Sculac

University of Split, Faculty of Science, Split, Croatia

M. Kovac, T. Sculac

Institute Rudjer Boskovic, Zagreb, Croatia

P. Bargassa, V. Brigljevic, B.K. Chitroda, D. Ferencek, S. Mishra, A. Starodumov[16], T. Susa

University of Cyprus, Nicosia, Cyprus

A. Attikis, K. Christoforou, S. Konstantinou, J. Mousa, C. Nicolaou, F. Ptochos, P.A. Razis, H. Rykaczewski, H. Saka, A. Stepennov

Charles University, Prague, Czech Republic

M. Finger, M. Finger Jr., A. Kveton

Escuela Politecnica Nacional, Quito, Ecuador

E. Ayala

Universidad San Francisco de Quito, Quito, Ecuador

E. Carrera Jarrin

Academy of Scientific Research and Technology of the Arab Republic of Egypt, Egyptian Network of High Energy Physics, Cairo, Egypt

H. Abdalla[17], Y. Assran[18,19]

Center for High Energy Physics (CHEP-FU), Fayoum University, El-Fayoum, Egypt

M.A. Mahmoud, Y. Mohammed

National Institute of Chemical Physics and Biophysics, Tallinn, Estonia

K. Ehataht, M. Kadastik, T. Lange, S. Nandan, C. Nielsen, J. Pata, M. Raidal, L. Tani, C. Veelken

Department of Physics, University of Helsinki, Helsinki, Finland

H. Kirschenmann, K. Osterberg, M. Voutilainen

Helsinki Institute of Physics, Helsinki, Finland

S. Bharthuar ![], E. Brücken ![], F. Garcia ![], K.T.S. Kallonen ![], R. Kinnunen, T. Lampén ![],
K. Lassila-Perini ![], S. Lehti ![], T. Lindén ![], L. Martikainen ![], M. Myllymäki ![], M.m. Rantanen ![],
H. Siikonen ![], E. Tuominen ![], J. Tuominiemi ![]

Lappeenranta-Lahti University of Technology, Lappeenranta, Finland

P. Luukka ![], H. Petrow ![]

IRFU, CEA, Université Paris-Saclay, Gif-sur-Yvette, France

M. Besancon ![], F. Couderc ![], M. Dejardin ![], D. Denegri, J.L. Faure, F. Ferri ![], S. Ganjour ![],
P. Gras ![], G. Hamel de Monchenault ![], V. Lohezic ![], J. Malcles ![], J. Rander, A. Rosowsky ![],
M.Ö. Sahin ![], A. Savoy-Navarro ![][20], P. Simkina ![], M. Titov ![], M. Tornago ![]

**Laboratoire Leprince-Ringuet, CNRS/IN2P3, Ecole Polytechnique, Institut
Polytechnique de Paris, Palaiseau, France**

C. Baldenegro Barrera ![], F. Beaudette ![], A. Buchot Perraguin ![], P. Busson ![], A. Cappati ![],
C. Charlot ![], M. Chiusi ![], F. Damas ![], O. Davignon ![], A. De Wit ![], B.A. Fontana Santos Alves ![],
S. Ghosh ![], A. Gilbert ![], R. Granier de Cassagnac ![], A. Hakimi ![], B. Harikrishnan ![],
L. Kalipoliti ![], G. Liu ![], J. Motta ![], M. Nguyen ![], C. Ochando ![], L. Portales ![], R. Salerno ![],
J.B. Sauvan ![], Y. Sirois ![], A. Tarabini ![], E. Vernazza ![], A. Zabi ![], A. Zghiche ![]

Université de Strasbourg, CNRS, IPHC UMR 7178, Strasbourg, France

J.-L. Agram ![][21], J. Andrea ![], D. Apparu ![], D. Bloch ![], J.-M. Brom ![], E.C. Chabert ![],
C. Collard ![], S. Falke ![], U. Goerlach ![], C. Grimault, R. Haeberle ![], A.-C. Le Bihan ![], M. Meena ![],
G. Saha ![], M.A. Sessini ![], P. Van Hove ![]

Institut de Physique des 2 Infinis de Lyon (IP2I), Villeurbanne, France

S. Beauceron ![], B. Blancon ![], G. Boudoul ![], N. Chanon ![], J. Choi ![], D. Contardo ![], P. Depasse ![],
C. Dozen ![][22], H. El Mamouni, J. Fay ![], S. Gascon ![], M. Gouzevitch ![], C. Greenberg, G. Grenier ![],
B. Ille ![], I.B. Laktineh, M. Lethuillier ![], L. Mirabito, S. Perries, A. Purohit ![], M. Vander Donckt ![],
P. Verdier ![], J. Xiao ![]

Georgian Technical University, Tbilisi, Georgia

I. Bagaturia ![][23], I. Lomidze ![], Z. Tsamalaidze ![][16]

RWTH Aachen University, I. Physikalisches Institut, Aachen, Germany

V. Botta ![], L. Feld ![], K. Klein ![], M. Lipinski ![], D. Meuser ![], A. Pauls ![], N. Röwert ![],
M. Teroerde ![]

RWTH Aachen University, III. Physikalisches Institut A, Aachen, Germany

S. Diekmann ![], A. Dodonova ![], N. Eich ![], D. Eliseev ![], F. Engelke ![], J. Erdmann, M. Erdmann ![],
P. Fackeldey ![], B. Fischer ![], T. Hebbeker ![], K. Hoepfner ![], F. Ivone ![], A. Jung ![], M.y. Lee ![],
L. Mastrolorenzo, F. Mausolf ![], M. Merschmeyer ![], A. Meyer ![], S. Mukherjee, D. Noll ![],
A. Novak ![], F. Nowotny, A. Pozdnyakov ![], Y. Rath, W. Redjeb ![], F. Rehm, H. Reithler ![],
U. Sarkar ![], V. Sarkisovi ![], A. Schmidt ![], A. Sharma ![], J.L. Spah ![], A. Stein ![],
F. Torres Da Silva De Araujo ![][24], L. Vigilante, S. Wiedenbeck ![], S. Zaleski

RWTH Aachen University, III. Physikalisches Institut B, Aachen, Germany

C. Dziwok [ORCID], G. Flügge [ORCID], W. Haj Ahmad [ORCID] [25], T. Kress [ORCID], A. Nowack [ORCID], O. Pooth [ORCID], A. Stahl [ORCID], T. Ziemons [ORCID], A. Zotz [ORCID]

Deutsches Elektronen-Synchrotron, Hamburg, Germany

H. Aarup Petersen [ORCID], M. Aldaya Martin [ORCID], J. Alimena [ORCID], S. Amoroso, Y. An [ORCID], S. Baxter [ORCID], M. Bayatmakou [ORCID], H. Becerril Gonzalez [ORCID], O. Behnke [ORCID], A. Belvedere [ORCID], S. Bhattacharya [ORCID], F. Blekman [ORCID] [26], K. Borras [ORCID] [27], A. Campbell [ORCID], A. Cardini [ORCID], C. Cheng, F. Colombina [ORCID], S. Consuegra Rodríguez [ORCID], G. Correia Silva [ORCID], M. De Silva [ORCID], G. Eckerlin, D. Eckstein [ORCID], L.I. Estevez Banos [ORCID], O. Filatov [ORCID], E. Gallo [ORCID] [26], A. Geiser [ORCID], A. Giraldi [ORCID], G. Greau, V. Guglielmi [ORCID], M. Guthoff [ORCID], A. Hinzmann [ORCID], A. Jafari [ORCID] [28], L. Jeppe [ORCID], N.Z. Jomhari [ORCID], B. Kaech [ORCID], M. Kasemann [ORCID], C. Kleinwort [ORCID], R. Kogler [ORCID], M. Komm [ORCID], D. Krücker [ORCID], W. Lange, D. Leyva Pernia [ORCID], K. Lipka [ORCID] [29], W. Lohmann [ORCID] [30], R. Mankel [ORCID], I.-A. Melzer-Pellmann [ORCID], M. Mendizabal Morentin [ORCID], A.B. Meyer [ORCID], G. Milella [ORCID], A. Mussgiller [ORCID], L.P. Nair [ORCID], A. Nürnberg [ORCID], Y. Otarid, J. Park [ORCID], D. Pérez Adán [ORCID], E. Ranken [ORCID], A. Raspereza [ORCID], B. Ribeiro Lopes [ORCID], J. Rübenach, A. Saggio [ORCID], M. Scham [ORCID] [31,27], S. Schnake [ORCID] [27], P. Schütze [ORCID], C. Schwanenberger [ORCID] [26], D. Selivanova [ORCID], K. Sharko [ORCID], M. Shchedrolosiev [ORCID], R.E. Sosa Ricardo [ORCID], D. Stafford, F. Vazzoler [ORCID], A. Ventura Barroso [ORCID], R. Walsh [ORCID], Q. Wang [ORCID], Y. Wen [ORCID], K. Wichmann, L. Wiens [ORCID] [27], C. Wissing [ORCID], Y. Yang [ORCID], A. Zimermmane Castro Santos [ORCID]

University of Hamburg, Hamburg, Germany

A. Albrecht [ORCID], S. Albrecht [ORCID], M. Antonello [ORCID], S. Bein [ORCID], L. Benato [ORCID], M. Bonanomi [ORCID], P. Connor [ORCID], M. Eich, K. El Morabit [ORCID], Y. Fischer [ORCID], A. Fröhlich, C. Garbers [ORCID], E. Garutti [ORCID], A. Grohsjean [ORCID], M. Hajheidari, J. Haller [ORCID], H.R. Jabusch [ORCID], G. Kasieczka [ORCID], P. Keicher, R. Klanner [ORCID], W. Korcari [ORCID], T. Kramer [ORCID], V. Kutzner [ORCID], F. Labe [ORCID], J. Lange [ORCID], A. Lobanov [ORCID], C. Matthies [ORCID], A. Mehta [ORCID], L. Moureaux [ORCID], M. Mrowietz, A. Nigamova [ORCID], Y. Nissan, A. Paasch [ORCID], K.J. Pena Rodriguez [ORCID], T. Quadfasel [ORCID], B. Raciti [ORCID], M. Rieger [ORCID], D. Savoiu [ORCID], J. Schindler, P. Schleper [ORCID], M. Schröder [ORCID], J. Schwandt [ORCID], M. Sommerhalder [ORCID], H. Stadie [ORCID], G. Steinbrück [ORCID], A. Tews, M. Wolf [ORCID]

Karlsruher Institut fuer Technologie, Karlsruhe, Germany

S. Brommer [ORCID], M. Burkart, E. Butz [ORCID], T. Chwalek [ORCID], A. Dierlamm [ORCID], A. Droll, N. Faltermann [ORCID], M. Giffels [ORCID], A. Gottmann [ORCID], F. Hartmann [ORCID] [32], R. Hofsaess [ORCID], M. Horzela [ORCID], U. Husemann [ORCID], J. Kieseler [ORCID], M. Klute [ORCID], R. Koppenhöfer [ORCID], J.M. Lawhorn [ORCID], M. Link, A. Lintuluoto [ORCID], S. Maier [ORCID], S. Mitra [ORCID], M. Mormile [ORCID], Th. Müller [ORCID], M. Neukum, M. Oh [ORCID], M. Presilla [ORCID], G. Quast [ORCID], K. Rabbertz [ORCID], B. Regnery [ORCID], N. Shadskiy [ORCID], I. Shvetsov, H.J. Simonis [ORCID], M. Toms [ORCID], N. Trevisani [ORCID], R. Ulrich [ORCID], R.F. Von Cube [ORCID], M. Wassmer [ORCID], S. Wieland [ORCID], F. Wittig, R. Wolf [ORCID], X. Zuo [ORCID]

Institute of Nuclear and Particle Physics (INPP), NCSR Demokritos, Aghia Paraskevi, Greece

G. Anagnostou, G. Daskalakis [ORCID], A. Kyriakis, A. Papadopoulos [32], A. Stakia [ORCID]

National and Kapodistrian University of Athens, Athens, Greece

P. Kontaxakis [ORCID], G. Melachroinos, A. Panagiotou, I. Papavergou [ORCID], I. Paraskevas [ORCID], N. Saoulidou [ORCID], K. Theofilatos [ORCID], E. Tziaferi [ORCID], K. Vellidis [ORCID], I. Zisopoulos [ORCID]

National Technical University of Athens, Athens, Greece

G. Bakas ©, T. Chatzistavrou, G. Karapostoli ©, K. Kousouris ©, I. Papakrivopoulos ©,
E. Siamarkou, G. Tsipolitis, A. Zacharopoulou

University of Ioánnina, Ioánnina, Greece

K. Adamidis, I. Bestintzanos, I. Evangelou ©, C. Foudas, C. Kamtsikis, P. Katsoulis, P. Kokkas ©,
P.G. Kosmoglou Kioseoglou ©, N. Manthos ©, I. Papadopoulos ©, J. Strologas ©

HUN-REN Wigner Research Centre for Physics, Budapest, Hungary

M. Bartók ©[33], C. Hajdu ©, D. Horvath ©[34,35], F. Sikler ©, V. Veszpremi ©

MTA-ELTE Lendület CMS Particle and Nuclear Physics Group, Eötvös Loránd University, Budapest, Hungary

M. Csanád ©, K. Farkas ©, M.M.A. Gadallah ©[36], Á. Kadlecsik ©, P. Major ©, K. Mandal ©,
G. Pásztor ©, A.J. Rádl ©[37], G.I. Veres ©

Faculty of Informatics, University of Debrecen, Debrecen, Hungary

P. Raics, B. Ujvari ©, G. Zilizi ©

Institute of Nuclear Research ATOMKI, Debrecen, Hungary

G. Bencze, S. Czellar, J. Molnar, Z. Szillasi

Karoly Robert Campus, MATE Institute of Technology, Gyongyos, Hungary

T. Csorgo ©[37], F. Nemes ©[37], T. Novak ©

Panjab University, Chandigarh, India

J. Babbar ©, S. Bansal ©, S.B. Beri, V. Bhatnagar ©, G. Chaudhary ©, S. Chauhan ©,
N. Dhingra ©[38], A. Kaur ©, A. Kaur ©, H. Kaur ©, M. Kaur ©, S. Kumar ©, K. Sandeep ©,
T. Sheokand, J.B. Singh ©, A. Singla ©

University of Delhi, Delhi, India

A. Ahmed ©, A. Bhardwaj ©, A. Chhetri ©, B.C. Choudhary ©, A. Kumar ©, A. Kumar ©,
M. Naimuddin ©, K. Ranjan, S. Saumya ©

Saha Institute of Nuclear Physics, HBNI, Kolkata, India

S. Baradia ©, S. Barman ©[39], S. Bhattacharya ©, S. Dutta ©, S. Dutta, S. Sarkar

Indian Institute of Technology Madras, Madras, India

M.M. Ameen ©, P.K. Behera ©, S.C. Behera ©, S. Chatterjee ©, P. Jana ©, P. Kalbhor ©,
J.R. Komaragiri ©[40], D. Kumar ©[40], L. Panwar ©[40], P.R. Pujahari ©, N.R. Saha ©, A. Sharma ©,
A.K. Sikdar ©, S. Verma ©

Tata Institute of Fundamental Research-A, Mumbai, India

S. Dugad, M. Kumar ©, G.B. Mohanty ©, P. Suryadevara

Tata Institute of Fundamental Research-B, Mumbai, India

A. Bala ©, S. Banerjee ©, R.M. Chatterjee, R.K. Dewanjee ©[41], M. Guchait ©, Sh. Jain ©,
S. Karmakar ©, S. Kumar ©, G. Majumder ©, K. Mazumdar ©, S. Parolia ©, A. Thachayath ©

National Institute of Science Education and Research, An OCC of Homi Bhabha National Institute, Bhubaneswar, Odisha, India

S. Bahinipati[42], C. Kar, D. Maity[43], P. Mal, T. Mishra,
V.K. Muraleedharan Nair Bindhu[43], K. Naskar[43], A. Nayak[43], P. Sadangi, P. Saha,
S.K. Swain, S. Varghese[43], D. Vats[43]

Indian Institute of Science Education and Research (IISER), Pune, India

S. Acharya[44], A. Alpana, S. Dube, B. Gomber[44], B. Kansal, A. Laha, B. Sahu[44],
S. Sharma

Isfahan University of Technology, Isfahan, Iran

H. Bakhshiansohi[45], E. Khazaie[46], M. Zeinali[47]

Institute for Research in Fundamental Sciences (IPM), Tehran, Iran

S. Chenarani[48], S.M. Etesami, M. Khakzad, M. Mohammadi Najafabadi

University College Dublin, Dublin, Ireland

M. Grunewald

INFN Sezione di Bari[a], Università di Bari[b], Politecnico di Bari[c], Bari, Italy

M. Abbrescia[a,b], R. Aly[a,c,49], A. Colaleo[a,b], D. Creanza[a,c], B. D'Anzi[a,b],
N. De Filippis[a,c], M. De Palma[a,b], A. Di Florio[a,c], W. Elmetenawee[a,b,49], L. Fiore[a],
G. Iaselli[a,c], M. Louka[a,b], G. Maggi[a,c], M. Maggi[a], I. Margjeka[a,b], V. Mastrapasqua[a,b],
S. My[a,b], S. Nuzzo[a,b], A. Pellecchia[a,b], A. Pompili[a,b], G. Pugliese[a,c], R. Radogna[a],
G. Ramirez-Sanchez[a,c], D. Ramos[a], A. Ranieri[a], L. Silvestris[a], F.M. Simone[a,b],
Ü. Sözbilir[a], A. Stamerra[a], R. Venditti[a], P. Verwilligen[a], A. Zaza[a,b]

INFN Sezione di Bologna[a], Università di Bologna[b], Bologna, Italy

G. Abbiendi[a], C. Battilana[a,b], D. Bonacorsi[a,b], L. Borgonovi[a], R. Campanini[a,b],
P. Capiluppi[a,b], F.R. Cavallo[a], M. Cuffiani[a,b], G.M. Dallavalle[a], T. Diotalevi[a,b],
F. Fabbri[a], A. Fanfani[a,b], D. Fasanella[a,b], P. Giacomelli[a], L. Giommi[a,b], C. Grandi[a],
L. Guiducci[a,b], S. Lo Meo[a,50], L. Lunerti[a,b], S. Marcellini[a], G. Masetti[a], F.L. Navarria[a,b],
A. Perrotta[a], F. Primavera[a,b], A.M. Rossi[a,b], T. Rovelli[a,b], G.P. Siroli[a,b]

INFN Sezione di Catania[a], Università di Catania[b], Catania, Italy

S. Costa[a,b,51], A. Di Mattia[a], R. Potenza[a,b], A. Tricomi[a,b,51], C. Tuve[a,b]

INFN Sezione di Firenze[a], Università di Firenze[b], Firenze, Italy

P. Assiouras[a], G. Barbagli[a], G. Bardelli[a,b], B. Camaiani[a,b], A. Cassese[a], R. Ceccarelli[a],
V. Ciulli[a,b], C. Civinini[a], R. D'Alessandro[a,b], E. Focardi[a,b], T. Kello[a], G. Latino[a,b],
P. Lenzi[a,b], M. Lizzo[a], M. Meschini[a], S. Paoletti[a], A. Papanastassiou[a,b], G. Sguazzoni[a],
L. Viliani[a]

INFN Laboratori Nazionali di Frascati, Frascati, Italy

L. Benussi, S. Bianco, S. Meola[52], D. Piccolo

INFN Sezione di Genova^a, Università di Genova^b, Genova, Italy

P. Chatagnon ⬡^a, F. Ferro ⬡^a, E. Robutti ⬡^a, S. Tosi ⬡^{a,b}

INFN Sezione di Milano-Bicocca^a, Università di Milano-Bicocca^b, Milano, Italy

A. Benaglia ⬡^a, G. Boldrini ⬡^{a,b}, F. Brivio ⬡^a, F. Cetorelli ⬡^a, F. De Guio ⬡^{a,b}, M.E. Dinardo ⬡^{a,b}, P. Dini ⬡^a, S. Gennai ⬡^a, R. Gerosa ⬡^{a,b}, A. Ghezzi ⬡^{a,b}, P. Govoni ⬡^{a,b}, L. Guzzi ⬡^a, M.T. Lucchini ⬡^{a,b}, M. Malberti ⬡^a, S. Malvezzi ⬡^a, A. Massironi ⬡^a, D. Menasce ⬡^a, L. Moroni ⬡^a, M. Paganoni ⬡^{a,b}, D. Pedrini ⬡^a, B.S. Pinolini^a, S. Ragazzi ⬡^{a,b}, T. Tabarelli de Fatis ⬡^{a,b}, D. Zuolo ⬡^a

INFN Sezione di Napoli^a, Università di Napoli 'Federico II'^b, Napoli, Italy; Università della Basilicata^c, Potenza, Italy; Scuola Superiore Meridionale (SSM)^d, Napoli, Italy

S. Buontempo ⬡^a, A. Cagnotta ⬡^{a,b}, F. Carnevali^{a,b}, N. Cavallo ⬡^{a,c}, A. De Iorio ⬡^{a,b}, F. Fabozzi ⬡^{a,c}, A.O.M. Iorio ⬡^{a,b}, L. Lista ⬡^{a,b,53}, P. Paolucci ⬡^{a,32}, B. Rossi ⬡^a, C. Sciacca ⬡^{a,b}

INFN Sezione di Padova^a, Università di Padova^b, Padova, Italy; Università di Trento^c, Trento, Italy

R. Ardino ⬡^a, P. Azzi ⬡^a, N. Bacchetta ⬡^{a,54}, D. Bisello ⬡^{a,b}, P. Bortignon ⬡^a, A. Bragagnolo ⬡^{a,b}, R. Carlin ⬡^{a,b}, P. Checchia ⬡^a, T. Dorigo ⬡^a, S. Fantinel ⬡^a, F. Fanzago ⬡^a, U. Gasparini ⬡^{a,b}, E. Lusiani ⬡^a, M. Margoni ⬡^{a,b}, F. Marini ⬡^a, A.T. Meneguzzo ⬡^{a,b}, M. Migliorini ⬡^{a,b}, J. Pazzini ⬡^{a,b}, P. Ronchese ⬡^{a,b}, R. Rossin ⬡^{a,b}, G. Strong ⬡^a, M. Tosi ⬡^{a,b}, A. Triossi ⬡^{a,b}, S. Ventura ⬡^a, H. Yarar^{a,b}, M. Zanetti ⬡^{a,b}, P. Zotto ⬡^{a,b}, A. Zucchetta ⬡^{a,b}, G. Zumerle ⬡^{a,b}

INFN Sezione di Pavia^a, Università di Pavia^b, Pavia, Italy

S. Abu Zeid ⬡^{a,55}, C. Aimè ⬡^{a,b}, A. Braghieri ⬡^a, S. Calzaferri ⬡^a, D. Fiorina ⬡^a, P. Montagna ⬡^{a,b}, V. Re ⬡^a, C. Riccardi ⬡^{a,b}, P. Salvini ⬡^a, I. Vai ⬡^{a,b}, P. Vitulo ⬡^{a,b}

INFN Sezione di Perugia^a, Università di Perugia^b, Perugia, Italy

S. Ajmal ⬡^{a,b}, G.M. Bilei ⬡^a, D. Ciangottini ⬡^{a,b}, L. Fanò ⬡^{a,b}, M. Magherini ⬡^{a,b}, G. Mantovani^{a,b}, V. Mariani ⬡^{a,b}, M. Menichelli ⬡^a, F. Moscatelli ⬡^{a,56}, A. Rossi ⬡^{a,b}, A. Santocchia ⬡^{a,b}, D. Spiga ⬡^a, T. Tedeschi ⬡^{a,b}

INFN Sezione di Pisa^a, Università di Pisa^b, Scuola Normale Superiore di Pisa^c, Pisa, Italy; Università di Siena^d, Siena, Italy

P. Asenov ⬡^{a,b}, P. Azzurri ⬡^a, G. Bagliesi ⬡^a, R. Bhattacharya ⬡^a, L. Bianchini ⬡^{a,b}, T. Boccali ⬡^a, E. Bossini ⬡^a, D. Bruschini ⬡^{a,c}, R. Castaldi ⬡^a, M.A. Ciocci ⬡^{a,b}, M. Cipriani ⬡^{a,b}, V. D'Amante ⬡^{a,d}, R. Dell'Orso ⬡^a, S. Donato ⬡^a, A. Giassi ⬡^a, F. Ligabue ⬡^{a,c}, D. Matos Figueiredo ⬡^a, A. Messineo ⬡^{a,b}, M. Musich ⬡^{a,b}, F. Palla ⬡^a, A. Rizzi ⬡^{a,b}, G. Rolandi ⬡^{a,c}, S. Roy Chowdhury ⬡^a, T. Sarkar ⬡^a, A. Scribano ⬡^a, P. Spagnolo ⬡^a, R. Tenchini ⬡^a, G. Tonelli ⬡^{a,b}, N. Turini ⬡^{a,d}, A. Venturi ⬡^a, P.G. Verdini ⬡^a

INFN Sezione di Roma^a, Sapienza Università di Roma^b, Roma, Italy

P. Barria ⬡^a, M. Campana ⬡^{a,b}, F. Cavallari ⬡^a, L. Cunqueiro Mendez ⬡^{a,b}, D. Del Re ⬡^{a,b}, E. Di Marco ⬡^a, M. Diemoz ⬡^a, F. Errico ⬡^{a,b}, E. Longo ⬡^{a,b}, P. Meridiani ⬡^a, J. Mijuskovic ⬡^{a,b},

G. Organtini [a,b], F. Pandolfi [a], R. Paramatti [a,b], C. Quaranta [a,b], S. Rahatlou [a,b], C. Rovelli [a], F. Santanastasio [a,b], L. Soffi [a]

INFN Sezione di Torino[a], Università di Torino[b], Torino, Italy; Università del Piemonte Orientale[c], Novara, Italy

N. Amapane [a,b], R. Arcidiacono [a,c], S. Argiro [a,b], M. Arneodo [a,c], N. Bartosik [a], R. Bellan [a,b], A. Bellora [a,b], C. Biino [a], C. Borca [a,b], N. Cartiglia [a], M. Costa [a,b], R. Covarelli [a,b], N. Demaria [a], L. Finco [a], M. Grippo [a,b], B. Kiani [a,b], F. Legger [a], F. Luongo [a,b], C. Mariotti [a], L. Markovic [a,b], S. Maselli [a], A. Mecca [a,b], E. Migliore [a,b], M. Monteno [a], R. Mulargia [a], M.M. Obertino [a,b], G. Ortona [a], L. Pacher [a,b], N. Pastrone [a], M. Pelliccioni [a], M. Ruspa [a,c], F. Siviero [a,b], V. Sola [a,b], A. Solano [a,b], A. Staiano [a], C. Tarricone [a,b], D. Trocino [a], G. Umoret [a,b], E. Vlasov [a,b]

INFN Sezione di Trieste[a], Università di Trieste[b], Trieste, Italy

S. Belforte [a], V. Candelise [a,b], M. Casarsa [a], F. Cossutti [a], K. De Leo [a,b], G. Della Ricca [a,b]

Kyungpook National University, Daegu, Korea

S. Dogra, J. Hong, C. Huh, B. Kim, D.H. Kim, J. Kim, H. Lee, S.W. Lee, C.S. Moon, Y.D. Oh, M.S. Ryu, S. Sekmen, Y.C. Yang

Department of Mathematics and Physics — GWNU, Gangneung, Korea

M.S. Kim

Chonnam National University, Institute for Universe and Elementary Particles, Kwangju, Korea

G. Bak, P. Gwak, H. Kim, D.H. Moon

Hanyang University, Seoul, Korea

E. Asilar, D. Kim, T.J. Kim, J.A. Merlin

Korea University, Seoul, Korea

S. Choi, S. Han, B. Hong, K. Lee, K.S. Lee, S. Lee, J. Park, S.K. Park, J. Yoo

Kyung Hee University, Department of Physics, Seoul, Korea

J. Goh, S. Yang

Sejong University, Seoul, Korea

H. S. Kim, Y. Kim, S. Lee

Seoul National University, Seoul, Korea

J. Almond, J.H. Bhyun, J. Choi, W. Jun, J. Kim, S. Ko, H. Kwon, H. Lee, J. Lee, J. Lee, B.H. Oh, S.B. Oh, H. Seo, U.K. Yang, I. Yoon

University of Seoul, Seoul, Korea

W. Jang, D.Y. Kang, Y. Kang, S. Kim, B. Ko, J.S.H. Lee, Y. Lee, I.C. Park, Y. Roh, I.J. Watson

Yonsei University, Department of Physics, Seoul, Korea

S. Ha , H.D. Yoo

Sungkyunkwan University, Suwon, Korea

M. Choi , M.R. Kim , H. Lee, Y. Lee , I. Yu

College of Engineering and Technology, American University of the Middle East (AUM), Dasman, Kuwait

T. Beyrouthy, Y. Maghrbi

Riga Technical University, Riga, Latvia

K. Dreimanis , A. Gaile , G. Pikurs, A. Potrebko , M. Seidel , V. Veckalns [57]

University of Latvia (LU), Riga, Latvia

N.R. Strautnieks

Vilnius University, Vilnius, Lithuania

M. Ambrozas , A. Juodagalvis , A. Rinkevicius , G. Tamulaitis

National Centre for Particle Physics, Universiti Malaya, Kuala Lumpur, Malaysia

N. Bin Norjoharuddeen , I. Yusuff [58], Z. Zolkapli

Universidad de Sonora (UNISON), Hermosillo, Mexico

J.F. Benitez , A. Castaneda Hernandez , H.A. Encinas Acosta, L.G. Gallegos Maríñez, M. León Coello , J.A. Murillo Quijada , A. Sehrawat , L. Valencia Palomo

Centro de Investigacion y de Estudios Avanzados del IPN, Mexico City, Mexico

G. Ayala , H. Castilla-Valdez , H. Crotte Ledesma, E. De La Cruz-Burelo , I. Heredia-De La Cruz [59], R. Lopez-Fernandez , C.A. Mondragon Herrera, A. Sánchez Hernández

Universidad Iberoamericana, Mexico City, Mexico

C. Oropeza Barrera , M. Ramírez García

Benemerita Universidad Autonoma de Puebla, Puebla, Mexico

I. Bautista , I. Pedraza , H.A. Salazar Ibarguen , C. Uribe Estrada

University of Montenegro, Podgorica, Montenegro

I. Bubanja, N. Raicevic

University of Canterbury, Christchurch, New Zealand

P.H. Butler

National Centre for Physics, Quaid-I-Azam University, Islamabad, Pakistan

A. Ahmad , M.I. Asghar, A. Awais , M.I.M. Awan, H.R. Hoorani , W.A. Khan

AGH University of Krakow, Faculty of Computer Science, Electronics and Telecommunications, Krakow, Poland

V. Avati, L. Grzanka ⓘ, M. Malawski ⓘ

National Centre for Nuclear Research, Swierk, Poland

H. Bialkowska ⓘ, M. Bluj ⓘ, B. Boimska ⓘ, M. Górski ⓘ, M. Kazana ⓘ, M. Szleper ⓘ, P. Zalewski ⓘ

Institute of Experimental Physics, Faculty of Physics, University of Warsaw, Warsaw, Poland

K. Bunkowski ⓘ, K. Doroba ⓘ, A. Kalinowski ⓘ, M. Konecki ⓘ, J. Krolikowski ⓘ, A. Muhammad ⓘ

Warsaw University of Technology, Warsaw, Poland

K. Pozniak ⓘ, W. Zabolotny ⓘ

Laboratório de Instrumentação e Física Experimental de Partículas, Lisboa, Portugal

M. Araujo ⓘ, D. Bastos ⓘ, C. Beirão Da Cruz E Silva ⓘ, A. Boletti ⓘ, M. Bozzo ⓘ, T. Camporesi ⓘ, G. Da Molin ⓘ, P. Faccioli ⓘ, M. Gallinaro ⓘ, J. Hollar ⓘ, N. Leonardo ⓘ, T. Niknejad ⓘ, A. Petrilli ⓘ, M. Pisano ⓘ, J. Seixas ⓘ, J. Varela ⓘ, J.W. Wulff

Faculty of Physics, University of Belgrade, Belgrade, Serbia

P. Adzic ⓘ, P. Milenovic ⓘ

VINCA Institute of Nuclear Sciences, University of Belgrade, Belgrade, Serbia

M. Dordevic ⓘ, J. Milosevic ⓘ, V. Rekovic

Centro de Investigaciones Energéticas Medioambientales y Tecnológicas (CIEMAT), Madrid, Spain

M. Aguilar-Benitez, J. Alcaraz Maestre ⓘ, Cristina F. Bedoya ⓘ, M. Cepeda ⓘ, M. Cerrada ⓘ, N. Colino ⓘ, B. De La Cruz ⓘ, A. Delgado Peris ⓘ, A. Escalante Del Valle ⓘ, D. Fernández Del Val ⓘ, J.P. Fernández Ramos ⓘ, J. Flix ⓘ, M.C. Fouz ⓘ, O. Gonzalez Lopez ⓘ, S. Goy Lopez ⓘ, J.M. Hernandez ⓘ, M.I. Josa ⓘ, D. Moran ⓘ, C. M. Morcillo Perez ⓘ, Á. Navarro Tobar ⓘ, C. Perez Dengra ⓘ, A. Pérez-Calero Yzquierdo ⓘ, J. Puerta Pelayo ⓘ, I. Redondo ⓘ, D.D. Redondo Ferrero ⓘ, L. Romero, S. Sánchez Navas ⓘ, L. Urda Gómez ⓘ, J. Vazquez Escobar ⓘ, C. Willmott

Universidad Autónoma de Madrid, Madrid, Spain

J.F. de Trocóniz ⓘ

Universidad de Oviedo, Instituto Universitario de Ciencias y Tecnologías Espaciales de Asturias (ICTEA), Oviedo, Spain

B. Alvarez Gonzalez ⓘ, J. Cuevas ⓘ, J. Fernandez Menendez ⓘ, S. Folgueras ⓘ, I. Gonzalez Caballero ⓘ, J.R. González Fernández ⓘ, E. Palencia Cortezon ⓘ, C. Ramón Álvarez ⓘ, V. Rodríguez Bouza ⓘ, A. Soto Rodríguez ⓘ, A. Trapote ⓘ, C. Vico Villalba ⓘ, P. Vischia ⓘ

Instituto de Física de Cantabria (IFCA), CSIC-Universidad de Cantabria, Santander, Spain

S. Bhowmik ©, S. Blanco Fernández ©, J.A. Brochero Cifuentes ©, I.J. Cabrillo ©, A. Calderon ©, J. Duarte Campderros ©, M. Fernandez ©, G. Gomez ©, C. Lasaosa García ©, C. Martinez Rivero ©, P. Martinez Ruiz del Arbol ©, F. Matorras ©, P. Matorras Cuevas ©, E. Navarrete Ramos ©, J. Piedra Gomez ©, L. Scodellaro ©, I. Vila ©, J.M. Vizan Garcia ©

University of Colombo, Colombo, Sri Lanka

M.K. Jayananda ©, B. Kailasapathy ©[60], D.U.J. Sonnadara ©, D.D.C. Wickramarathna ©

University of Ruhuna, Department of Physics, Matara, Sri Lanka

W.G.D. Dharmaratna ©[61], K. Liyanage ©, N. Perera ©, N. Wickramage ©

CERN, European Organization for Nuclear Research, Geneva, Switzerland

D. Abbaneo ©, C. Amendola ©, E. Auffray ©, G. Auzinger ©, J. Baechler, D. Barney ©, A. Bermúdez Martínez ©, M. Bianco ©, B. Bilin ©, A.A. Bin Anuar ©, A. Bocci ©, C. Botta ©, E. Brondolin ©, C. Caillol ©, G. Cerminara ©, N. Chernyavskaya ©, D. d'Enterria ©, A. Dabrowski ©, A. David ©, A. De Roeck ©, M.M. Defranchis ©, M. Deile ©, M. Dobson ©, L. Forthomme ©, G. Franzoni ©, W. Funk ©, S. Giani, D. Gigi, K. Gill ©, F. Glege ©, L. Gouskos ©, M. Haranko ©, J. Hegeman ©, B. Huber, V. Innocente ©, T. James ©, P. Janot ©, S. Laurila ©, P. Lecoq ©, E. Leutgeb ©, C. Lourenço ©, B. Maier ©, L. Malgeri ©, M. Mannelli ©, A.C. Marini ©, M. Matthewman, F. Meijers ©, S. Mersi ©, E. Meschi ©, V. Milosevic, F. Monti ©, F. Moortgat ©, M. Mulders ©, I. Neutelings ©, S. Orfanelli, F. Pantaleo ©, G. Petrucciani ©, A. Pfeiffer ©, M. Pierini ©, D. Piparo ©, H. Qu ©, D. Rabady ©, G. Reales Gutiérrez, M. Rovere ©, H. Sakulin ©, S. Scarfi ©, C. Schwick, M. Selvaggi ©, A. Sharma ©, K. Shchelina ©, P. Silva ©, P. Sphicas ©[62], A.G. Stahl Leiton ©, A. Steen ©, S. Summers ©, D. Treille ©, P. Tropea ©, A. Tsirou, D. Walter ©, J. Wanczyk ©[63], J. Wang, S. Wuchterl ©, P. Zehetner ©, P. Zejdl ©, W.D. Zeuner

Paul Scherrer Institut, Villigen, Switzerland

T. Bevilacqua ©[64], L. Caminada ©[64], A. Ebrahimi ©, W. Erdmann ©, R. Horisberger ©, Q. Ingram ©, H.C. Kaestli ©, D. Kotlinski ©, C. Lange ©, M. Missiroli ©[64], L. Noehte ©[64], T. Rohe ©

ETH Zurich — Institute for Particle Physics and Astrophysics (IPA), Zurich, Switzerland

T.K. Aarrestad ©, K. Androsov ©[63], M. Backhaus ©, A. Calandri ©, C. Cazzaniga ©, K. Datta ©, A. De Cosa ©, G. Dissertori ©, M. Dittmar, M. Donegà ©, F. Eble ©, M. Galli ©, K. Gedia ©, F. Glessgen ©, C. Grab ©, D. Hits ©, W. Lustermann ©, A.-M. Lyon ©, R.A. Manzoni ©, M. Marchegiani ©, L. Marchese ©, C. Martin Perez ©, A. Mascellani ©[63], F. Nessi-Tedaldi ©, F. Pauss ©, V. Perovic, S. Pigazzini ©, C. Reissel ©, T. Reitenspiess ©, B. Ristic, F. Riti ©, D. Ruini, R. Seidita ©, J. Steggemann ©[63], D. Valsecchi ©, R. Wallny ©

Universität Zürich, Zurich, Switzerland

C. Amsler ©[65], P. Bärtschi ©, D. Brzhechko, M.F. Canelli ©, K. Cormier ©, J.K. Heikkilä ©, M. Huwiler ©, W. Jin ©, A. Jofrehei ©, B. Kilminster ©, S. Leontsinis ©, S.P. Liechti ©,

A. Macchiolo [⬚], P. Meiring [⬚], U. Molinatti [⬚], A. Reimers [⬚], P. Robmann, S. Sanchez Cruz [⬚],
M. Senger [⬚], Y. Takahashi [⬚], R. Tramontano [⬚]

National Central University, Chung-Li, Taiwan

C. Adloff[66], D. Bhowmik, C.M. Kuo, W. Lin, P.K. Rout [⬚], P.C. Tiwari [⬚][40], S.S. Yu [⬚]

National Taiwan University (NTU), Taipei, Taiwan

L. Ceard, Y. Chao [⬚], K.F. Chen [⬚], P.s. Chen, Z.g. Chen, W.-S. Hou [⬚], T.h. Hsu, Y.w. Kao,
R. Khurana, G. Kole [⬚], Y.y. Li [⬚], R.-S. Lu [⬚], E. Paganis [⬚], X.f. Su, J. Thomas-Wilsker [⬚], L.s. Tsai,
H.y. Wu, E. Yazgan [⬚]

High Energy Physics Research Unit, Department of Physics, Faculty of Science, Chulalongkorn University, Bangkok, Thailand

C. Asawatangtrakuldee [⬚], N. Srimanobhas [⬚], V. Wachirapusitanand [⬚]

Çukurova University, Physics Department, Science and Art Faculty, Adana, Turkey

D. Agyel [⬚], F. Boran [⬚], Z.S. Demiroglu [⬚], F. Dolek [⬚], I. Dumanoglu [⬚][67], E. Eskut [⬚], Y. Guler [⬚][68],
E. Gurpinar Guler [⬚][68], C. Isik [⬚], O. Kara, A. Kayis Topaksu [⬚], U. Kiminsu [⬚], G. Onengut [⬚],
K. Ozdemir [⬚][69], A. Polatoz [⬚], B. Tali [⬚][70], U.G. Tok [⬚], S. Turkcapar [⬚], E. Uslan [⬚], I.S. Zorbakir [⬚]

Middle East Technical University, Physics Department, Ankara, Turkey

M. Yalvac [⬚][71]

Bogazici University, Istanbul, Turkey

B. Akgun [⬚], I.O. Atakisi [⬚], E. Gülmez [⬚], M. Kaya [⬚][72], O. Kaya [⬚][73], S. Tekten [⬚][74]

Istanbul Technical University, Istanbul, Turkey

A. Cakir [⬚], K. Cankocak [⬚][67,75], Y. Komurcu, S. Sen [⬚][76]

Istanbul University, Istanbul, Turkey

O. Aydilek [⬚], S. Cerci [⬚][70], V. Epshteyn [⬚], B. Hacisahinoglu [⬚], I. Hos [⬚][77], B. Kaynak [⬚],
S. Ozkorucuklu [⬚], O. Potok [⬚], H. Sert [⬚], C. Simsek [⬚], C. Zorbilmez [⬚]

Yildiz Technical University, Istanbul, Turkey

B. Isildak [⬚][78], D. Sunar Cerci [⬚][70]

Institute for Scintillation Materials of National Academy of Science of Ukraine, Kharkiv, Ukraine

A. Boyaryntsev [⬚], B. Grynyov [⬚]

National Science Centre, Kharkiv Institute of Physics and Technology, Kharkiv, Ukraine

L. Levchuk [⬚]

University of Bristol, Bristol, United Kingdom

D. Anthony ⓘ, J.J. Brooke ⓘ, A. Bundock ⓘ, F. Bury ⓘ, E. Clement ⓘ, D. Cussans ⓘ, H. Flacher ⓘ,
M. Glowacki, J. Goldstein ⓘ, H.F. Heath ⓘ, L. Kreczko ⓘ, S. Paramesvaran ⓘ, S. Seif El Nasr-Storey,
V.J. Smith ⓘ, N. Stylianou ⓘ[79], K. Walkingshaw Pass, R. White ⓘ

Rutherford Appleton Laboratory, Didcot, United Kingdom

A.H. Ball, K.W. Bell ⓘ, A. Belyaev ⓘ[80], C. Brew ⓘ, R.M. Brown ⓘ, D.J.A. Cockerill ⓘ, C. Cooke ⓘ,
K.V. Ellis, K. Harder ⓘ, S. Harper ⓘ, M.-L. Holmberg ⓘ[81], J. Linacre ⓘ, K. Manolopoulos,
D.M. Newbold ⓘ, E. Olaiya, D. Petyt ⓘ, T. Reis ⓘ, G. Salvi ⓘ, T. Schuh,
C.H. Shepherd-Themistocleous ⓘ, I.R. Tomalin ⓘ, T. Williams ⓘ

Imperial College, London, United Kingdom

R. Bainbridge ⓘ, P. Bloch ⓘ, C.E. Brown ⓘ, O. Buchmuller, V. Cacchio, C.A. Carrillo Montoya ⓘ,
V. Cepaitis ⓘ, G.S. Chahal ⓘ[82], D. Colling ⓘ, J.S. Dancu, I. Das ⓘ, P. Dauncey ⓘ, G. Davies ⓘ,
J. Davies, M. Della Negra ⓘ, S. Fayer, G. Fedi ⓘ, G. Hall ⓘ, M.H. Hassanshahi ⓘ, A. Howard,
G. Iles ⓘ, M. Knight ⓘ, J. Langford ⓘ, J. León Holgado ⓘ, L. Lyons ⓘ, A.-M. Magnan ⓘ, S. Malik,
M. Mieskolainen ⓘ, J. Nash ⓘ[83], M. Pesaresi, B.C. Radburn-Smith ⓘ, A. Richards, A. Rose ⓘ,
K. Savva, C. Seez ⓘ, R. Shukla ⓘ, A. Tapper ⓘ, K. Uchida ⓘ, G.P. Uttley ⓘ, L.H. Vage,
T. Virdee ⓘ[32], M. Vojinovic ⓘ, N. Wardle ⓘ, D. Winterbottom

Brunel University, Uxbridge, United Kingdom

K. Coldham, J.E. Cole ⓘ, A. Khan, P. Kyberd ⓘ, I.D. Reid ⓘ

Baylor University, Waco, Texas, U.S.A.

S. Abdullin ⓘ, A. Brinkerhoff ⓘ, B. Caraway ⓘ, J. Dittmann ⓘ, K. Hatakeyama ⓘ, J. Hiltbrand ⓘ,
B. McMaster ⓘ, M. Saunders ⓘ, S. Sawant ⓘ, C. Sutantawibul ⓘ, J. Wilson ⓘ

Catholic University of America, Washington, DC, U.S.A.

R. Bartek ⓘ, A. Dominguez ⓘ, C. Huerta Escamilla, A.E. Simsek ⓘ, R. Uniyal ⓘ,
A.M. Vargas Hernandez ⓘ

The University of Alabama, Tuscaloosa, Alabama, U.S.A.

B. Bam ⓘ, R. Chudasama ⓘ, S.I. Cooper ⓘ, S.V. Gleyzer ⓘ, C.U. Perez ⓘ, P. Rumerio ⓘ[84],
E. Usai ⓘ, R. Yi ⓘ

Boston University, Boston, Massachusetts, U.S.A.

A. Akpinar ⓘ, D. Arcaro ⓘ, C. Cosby ⓘ, Z. Demiragli ⓘ, C. Erice ⓘ, C. Fangmeier ⓘ,
C. Fernandez Madrazo ⓘ, E. Fontanesi ⓘ, D. Gastler ⓘ, F. Golf ⓘ, S. Jeon ⓘ, I. Reed ⓘ, J. Rohlf ⓘ,
K. Salyer ⓘ, D. Sperka ⓘ, D. Spitzbart ⓘ, I. Suarez ⓘ, A. Tsatsos ⓘ, S. Yuan ⓘ, A.G. Zecchinelli ⓘ

Brown University, Providence, Rhode Island, U.S.A.

G. Benelli ⓘ, X. Coubez[27], D. Cutts ⓘ, M. Hadley ⓘ, U. Heintz ⓘ, J.M. Hogan ⓘ[85], T. Kwon ⓘ,
G. Landsberg ⓘ, K.T. Lau ⓘ, D. Li ⓘ, J. Luo ⓘ, S. Mondal ⓘ, M. Narain ⓘ[†], N. Pervan ⓘ,
S. Sagir ⓘ[86], F. Simpson ⓘ, M. Stamenkovic ⓘ, W.Y. Wong, X. Yan ⓘ, W. Zhang

University of California, Davis, Davis, California, U.S.A.

S. Abbott , J. Bonilla , C. Brainerd , R. Breedon , M. Calderon De La Barca Sanchez , M. Chertok , M. Citron , J. Conway , P.T. Cox , R. Erbacher , F. Jensen , O. Kukral , G. Mocellin , M. Mulhearn , D. Pellett , W. Wei , Y. Yao , F. Zhang

University of California, Los Angeles, California, U.S.A.

M. Bachtis , R. Cousins , A. Datta , G. Flores Avila , J. Hauser , M. Ignatenko , M.A. Iqbal , T. Lam , E. Manca , A. Nunez Del Prado, D. Saltzberg , V. Valuev

University of California, Riverside, Riverside, California, U.S.A.

R. Clare , J.W. Gary , M. Gordon, G. Hanson , W. Si , S. Wimpenny [†]

University of California, San Diego, La Jolla, California, U.S.A.

J.G. Branson , S. Cittolin , S. Cooperstein , D. Diaz , J. Duarte , L. Giannini , J. Guiang , R. Kansal , V. Krutelyov , R. Lee , J. Letts , M. Masciovecchio , F. Mokhtar , S. Mukherjee , M. Pieri , M. Quinnan , B.V. Sathia Narayanan , V. Sharma , M. Tadel , E. Vourliotis , F. Würthwein , Y. Xiang , A. Yagil

University of California, Santa Barbara — Department of Physics, Santa Barbara, California, U.S.A.

A. Barzdukas , L. Brennan , C. Campagnari , A. Dorsett , J. Incandela , J. Kim , A.J. Li , P. Masterson , H. Mei , J. Richman , U. Sarica , R. Schmitz , F. Setti , J. Sheplock , D. Stuart , T.Á. Vámi , S. Wang

California Institute of Technology, Pasadena, California, U.S.A.

A. Bornheim , O. Cerri, A. Latorre, J. Mao , H.B. Newman , M. Spiropulu , J.R. Vlimant , C. Wang , S. Xie , R.Y. Zhu

Carnegie Mellon University, Pittsburgh, Pennsylvania, U.S.A.

J. Alison , S. An , M.B. Andrews , P. Bryant , M. Cremonesi, V. Dutta , T. Ferguson , A. Harilal , C. Liu , T. Mudholkar , S. Murthy , P. Palit , M. Paulini , A. Roberts , A. Sanchez , W. Terrill

University of Colorado Boulder, Boulder, Colorado, U.S.A.

J.P. Cumalat , W.T. Ford , A. Hassani , G. Karathanasis , E. MacDonald, N. Manganelli , A. Perloff , C. Savard , N. Schonbeck , K. Stenson , K.A. Ulmer , S.R. Wagner , N. Zipper

Cornell University, Ithaca, New York, U.S.A.

J. Alexander , S. Bright-Thonney , X. Chen , D.J. Cranshaw , J. Fan , X. Fan , D. Gadkari , S. Hogan , P. Kotamnives, J. Monroy , M. Oshiro , J.R. Patterson , J. Reichert , M. Reid , A. Ryd , J. Thom , P. Wittich , R. Zou

Fermi National Accelerator Laboratory, Batavia, Illinois, U.S.A.

M. Albrow , M. Alyari , O. Amram , G. Apollinari , A. Apresyan , L.A.T. Bauerdick , D. Berry , J. Berryhill , P.C. Bhat , K. Burkett , J.N. Butler , A. Canepa , G.B. Cerati , H.W.K. Cheung , F. Chlebana , G. Cummings , J. Dickinson , I. Dutta , V.D. Elvira ,

Y. Feng, J. Freeman, A. Gandrakota, Z. Gecse, L. Gray, D. Green, A. Grummer, S. Grünendahl, D. Guerrero, O. Gutsche, R.M. Harris, R. Heller, T.C. Herwig, J. Hirschauer, L. Horyn, B. Jayatilaka, S. Jindariani, M. Johnson, U. Joshi, T. Klijnsma, B. Klima, K.H.M. Kwok, S. Lammel, D. Lincoln, R. Lipton, T. Liu, C. Madrid, K. Maeshima, C. Mantilla, D. Mason, P. McBride, P. Merkel, S. Mrenna, S. Nahn, J. Ngadiuba, D. Noonan, V. Papadimitriou, N. Pastika, K. Pedro, C. Pena[87], F. Ravera, A. Reinsvold Hall[88], L. Ristori, E. Sexton-Kennedy, N. Smith, A. Soha, L. Spiegel, S. Stoynev, J. Strait, L. Taylor, S. Tkaczyk, N.V. Tran, L. Uplegger, E.W. Vaandering, I. Zoi

University of Florida, Gainesville, Florida, U.S.A.
C. Aruta, P. Avery, D. Bourilkov, L. Cadamuro, P. Chang, V. Cherepanov, R.D. Field, E. Koenig, M. Kolosova, J. Konigsberg, A. Korytov, K.H. Lo, K. Matchev, N. Menendez, G. Mitselmakher, K. Mohrman, A. Muthirakalayil Madhu, N. Rawal, D. Rosenzweig, S. Rosenzweig, K. Shi, J. Wang

Florida State University, Tallahassee, Florida, U.S.A.
T. Adams, A. Al Kadhim, A. Askew, S. Bower, R. Habibullah, V. Hagopian, R. Hashmi, R.S. Kim, S. Kim, T. Kolberg, G. Martinez, H. Prosper, P.R. Prova, M. Wulansatiti, R. Yohay, J. Zhang

Florida Institute of Technology, Melbourne, Florida, U.S.A.
B. Alsufyani, M.M. Baarmand, S. Butalla, T. Elkafrawy[55], M. Hohlmann, R. Kumar Verma, M. Rahmani, E. Yanes

University of Illinois Chicago, Chicago, U.S.A., Chicago, U.S.A.
M.R. Adams, A. Baty, C. Bennett, R. Cavanaugh, R. Escobar Franco, O. Evdokimov, C.E. Gerber, D.J. Hofman, J.h. Lee, D. S. Lemos, A.H. Merrit, C. Mills, S. Nanda, G. Oh, B. Ozek, D. Pilipovic, R. Pradhan, T. Roy, S. Rudrabhatla, M.B. Tonjes, N. Varelas, Z. Ye, J. Yoo

The University of Iowa, Iowa City, Iowa, U.S.A.
M. Alhusseini, D. Blend, K. Dilsiz[89], L. Emediato, G. Karaman, O.K. Köseyan, J.-P. Merlo, A. Mestvirishvili[90], J. Nachtman, O. Neogi, H. Ogul[91], Y. Onel, A. Penzo, C. Snyder, E. Tiras[92]

Johns Hopkins University, Baltimore, Maryland, U.S.A.
B. Blumenfeld, L. Corcodilos, J. Davis, A.V. Gritsan, L. Kang, S. Kyriacou, P. Maksimovic, M. Roguljic, J. Roskes, S. Sekhar, M. Swartz

The University of Kansas, Lawrence, Kansas, U.S.A.
A. Abreu, L.F. Alcerro Alcerro, J. Anguiano, P. Baringer, A. Bean, Z. Flowers, D. Grove, J. King, G. Krintiras, M. Lazarovits, C. Le Mahieu, C. Lindsey, J. Marquez, N. Minafra, M. Murray, M. Nickel, M. Pitt, S. Popescu[93], C. Rogan, C. Royon, R. Salvatico, S. Sanders, C. Smith, Q. Wang, G. Wilson

Kansas State University, Manhattan, Kansas, U.S.A.

B. Allmond [●], A. Ivanov [●], K. Kaadze [●], A. Kalogeropoulos [●], D. Kim, Y. Maravin [●], K. Nam, J. Natoli [●], D. Roy [●], G. Sorrentino [●]

Lawrence Livermore National Laboratory, Livermore, California, U.S.A.

F. Rebassoo [●], D. Wright [●]

University of Maryland, College Park, Maryland, U.S.A.

A. Baden [●], A. Belloni [●], Y.M. Chen [●], S.C. Eno [●], N.J. Hadley [●], S. Jabeen [●], R.G. Kellogg [●], T. Koeth [●], Y. Lai [●], S. Lascio [●], A.C. Mignerey [●], S. Nabili [●], C. Palmer [●], C. Papageorgakis [●], M.M. Paranjpe, L. Wang [●]

Massachusetts Institute of Technology, Cambridge, Massachusetts, U.S.A.

J. Bendavid [●], W. Busza [●], I.A. Cali [●], M. D'Alfonso [●], J. Eysermans [●], C. Freer [●], G. Gomez-Ceballos [●], M. Goncharov, G. Grosso, P. Harris, D. Hoang, D. Kovalskyi [●], J. Krupa [●], L. Lavezzo [●], Y.-J. Lee [●], K. Long [●], C. Mironov [●], C. Paus [●], D. Rankin [●], C. Roland [●], G. Roland [●], S. Rothman [●], G.S.F. Stephans [●], Z. Wang [●], B. Wyslouch [●], T. J. Yang [●]

University of Minnesota, Minneapolis, Minnesota, U.S.A.

B. Crossman [●], B.M. Joshi [●], C. Kapsiak [●], M. Krohn [●], D. Mahon [●], J. Mans [●], B. Marzocchi [●], S. Pandey [●], M. Revering [●], R. Rusack [●], R. Saradhy [●], N. Schroeder [●], N. Strobbe [●], M.A. Wadud [●]

**University of Mississippi, Oxford, Mississippi, U.S.A.**

L.M. Cremaldi [●]

University of Nebraska-Lincoln, Lincoln, Nebraska, U.S.A.

K. Bloom [●], D.R. Claes [●], G. Haza [●], J. Hossain [●], C. Joo [●], I. Kravchenko [●], J.E. Siado [●], W. Tabb [●], A. Vagnerini [●], A. Wightman [●], F. Yan [●], D. Yu [●]

State University of New York at Buffalo, Buffalo, New York, U.S.A.

H. Bandyopadhyay [●], L. Hay [●], I. Iashvili [●], A. Kharchilava [●], M. Morris [●], D. Nguyen [●], S. Rappoccio [●], H. Rejeb Sfar, A. Williams [●]

Northeastern University, Boston, Massachusetts, U.S.A.

G. Alverson [●], E. Barberis [●], J. Dervan, Y. Haddad [●], Y. Han [●], A. Krishna [●], J. Li [●], M. Lu [●], G. Madigan [●], R. Mccarthy [●], D.M. Morse [●], V. Nguyen [●], T. Orimoto [●], A. Parker [●], L. Skinnari [●], A. Tishelman-Charny [●], B. Wang [●], D. Wood [●]

Northwestern University, Evanston, Illinois, U.S.A.

S. Bhattacharya [●], J. Bueghly, Z. Chen [●], S. Dittmer [●], K.A. Hahn [●], Y. Liu [●], Y. Miao [●], D.G. Monk [●], M.H. Schmitt [●], A. Taliercio [●], M. Velasco

**University of Notre Dame, Notre Dame, Indiana, U.S.A.**

G. Agarwal [●], R. Band [●], R. Bucci, S. Castells, A. Das [●], R. Goldouzian [●], M. Hildreth [●], K.W. Ho [●], K. Hurtado Anampa [●], T. Ivanov [●], C. Jessop [●], K. Lannon [●], J. Lawrence [●],

N. Loukas, L. Lutton, J. Mariano, N. Marinelli, I. Mcalister, T. McCauley, C. Mcgrady,
C. Moore, Y. Musienko[16], H. Nelson, M. Osherson, A. Piccinelli, R. Ruchti,
A. Townsend, Y. Wan, M. Wayne, H. Yockey, M. Zarucki, L. Zygala

The Ohio State University, Columbus, Ohio, U.S.A.
A. Basnet, B. Bylsma, M. Carrigan, L.S. Durkin, C. Hill, M. Joyce, M. Nunez Ornelas,
K. Wei, B.L. Winer, B. R. Yates

Princeton University, Princeton, New Jersey, U.S.A.
F.M. Addesa, H. Bouchamaoui, P. Das, G. Dezoort, P. Elmer, A. Frankenthal,
B. Greenberg, N. Haubrich, G. Kopp, S. Kwan, D. Lange, A. Loeliger, D. Marlow,
I. Ojalvo, J. Olsen, A. Shevelev, D. Stickland, C. Tully

University of Puerto Rico, Mayaguez, Puerto Rico, U.S.A.
S. Malik

Purdue University, West Lafayette, Indiana, U.S.A.
A.S. Bakshi, V.E. Barnes, S. Chandra, R. Chawla, S. Das, A. Gu, L. Gutay,
M. Jones, A.W. Jung, D. Kondratyev, A.M. Koshy, M. Liu, G. Negro, N. Neumeister,
G. Paspalaki, S. Piperov, V. Scheurer, J.F. Schulte, M. Stojanovic, J. Thieman,
A. K. Virdi, F. Wang, W. Xie

Purdue University Northwest, Hammond, Indiana, U.S.A.
J. Dolen, N. Parashar, A. Pathak

Rice University, Houston, Texas, U.S.A.
D. Acosta, T. Carnahan, K.M. Ecklund, P.J. Fernández Manteca, S. Freed, P. Gardner,
F.J.M. Geurts, W. Li, O. Miguel Colin, B.P. Padley, R. Redjimi, J. Rotter, E. Yigitbasi,
Y. Zhang

University of Rochester, Rochester, New York, U.S.A.
A. Bodek, P. de Barbaro, R. Demina, J.L. Dulemba, A. Garcia-Bellido, O. Hindrichs,
A. Khukhunaishvili, N. Parmar, P. Parygin[94], E. Popova[94], R. Taus

The Rockefeller University, New York, New York, U.S.A.
K. Goulianos

Rutgers, The State University of New Jersey, Piscataway, New Jersey, U.S.A.
B. Chiarito, J.P. Chou, Y. Gershtein, E. Halkiadakis, A. Hart, M. Heindl,
D. Jaroslawski, O. Karacheban[30], I. Laflotte, A. Lath, R. Montalvo, K. Nash, H. Routray,
S. Salur, S. Schnetzer, S. Somalwar, R. Stone, S.A. Thayil, S. Thomas, J. Vora,
H. Wang

University of Tennessee, Knoxville, Tennessee, U.S.A.
H. Acharya, D. Ally, A.G. Delannoy, S. Fiorendi, S. Higginbotham, T. Holmes,
A.R. Kanuganti, N. Karunarathna, L. Lee, E. Nibigira, S. Spanier

Texas A&M University, College Station, Texas, U.S.A.

D. Aebi ©, M. Ahmad ©, O. Bouhali ©[95], R. Eusebi ©, J. Gilmore ©, T. Huang ©, T. Kamon ©[96], H. Kim ©, S. Luo ©, R. Mueller ©, D. Overton ©, D. Rathjens ©, A. Safonov ©

Texas Tech University, Lubbock, Texas, U.S.A.

N. Akchurin ©, J. Damgov ©, V. Hegde ©, A. Hussain ©, Y. Kazhykarim, K. Lamichhane ©, S.W. Lee ©, A. Mankel ©, T. Peltola ©, I. Volobouev ©, A. Whitbeck ©

Vanderbilt University, Nashville, Tennessee, U.S.A.

E. Appelt ©, Y. Chen ©, S. Greene, A. Gurrola ©, W. Johns ©, R. Kunnawalkam Elayavalli ©, A. Melo ©, F. Romeo ©, P. Sheldon ©, S. Tuo ©, J. Velkovska ©, J. Viinikainen ©

University of Virginia, Charlottesville, Virginia, U.S.A.

B. Cardwell ©, B. Cox ©, J. Hakala ©, R. Hirosky ©, A. Ledovskoy ©, C. Neu ©, C.E. Perez Lara ©

Wayne State University, Detroit, Michigan, U.S.A.

P.E. Karchin ©

University of Wisconsin — Madison, Madison, Wisconsin, U.S.A.

A. Aravind, S. Banerjee ©, K. Black ©, T. Bose ©, S. Dasu ©, I. De Bruyn ©, P. Everaerts ©, C. Galloni, H. He ©, M. Herndon ©, A. Herve ©, C.K. Koraka ©, A. Lanaro, R. Loveless ©, J. Madhusudanan Sreekala ©, A. Mallampalli ©, A. Mohammadi ©, S. Mondal, G. Parida ©, D. Pinna, A. Savin, V. Shang ©, V. Sharma ©, W.H. Smith ©, D. Teague, H.F. Tsoi ©, W. Vetens ©, A. Warden ©

Authors affiliated with an institute or an international laboratory covered by a cooperation agreement with CERN

S. Afanasiev ©, V. Andreev ©, Yu. Andreev ©, T. Aushev ©, M. Azarkin ©, A. Babaev ©, A. Belyaev ©, V. Blinov[97], E. Boos ©, V. Borshch ©, D. Budkouski ©, V. Bunichev ©, M. Chadeeva ©[97], V. Chekhovsky, R. Chistov ©[97], A. Dermenev ©, T. Dimova ©[97], D. Druzhkin ©[98], M. Dubinin ©[87], L. Dudko ©, A. Ershov ©, G. Gavrilov ©, V. Gavrilov ©, S. Gninenko ©, V. Golovtcov ©, N. Golubev ©, I. Golutvin ©, I. Gorbunov ©, A. Gribushin ©, Y. Ivanov ©, V. Kachanov ©, V. Karjavine ©, A. Karneyeu ©, V. Kim ©[97], M. Kirakosyan, D. Kirpichnikov ©, M. Kirsanov ©, V. Klyukhin ©, O. Kodolova ©[99], V. Korenkov ©, A. Kozyrev ©[97], N. Krasnikov ©, A. Lanev ©, P. Levchenko ©[100], N. Lychkovskaya ©, V. Makarenko ©, A. Malakhov ©, V. Matveev ©[97], V. Murzin ©, A. Nikitenko ©[101,99], S. Obraztsov ©, V. Oreshkin ©, V. Palichik ©, V. Perelygin ©, M. Perfilov, S. Petrushanko ©, S. Polikarpov ©[97], V. Popov ©, O. Radchenko ©[97], M. Savina ©, V. Savrin ©, V. Shalaev ©, S. Shmatov ©, S. Shulha ©, Y. Skovpen ©[97], S. Slabospitskii ©, V. Smirnov ©, D. Sosnov ©, V. Sulimov ©, E. Tcherniaev ©, A. Terkulov ©, O. Teryaev ©, I. Tlisova ©, A. Toropin ©, L. Uvarov ©, A. Uzunian ©, A. Vorobyev[†], N. Voytishin ©, B.S. Yuldashev[102], A. Zarubin ©, I. Zhizhin ©, A. Zhokin ©

[†] *Deceased*

[1] *Also at Yerevan State University, Yerevan, Armenia*

[2] *Also at TU Wien, Vienna, Austria*

[3] *Also at Institute of Basic and Applied Sciences, Faculty of Engineering, Arab Academy for Science, Technology and Maritime Transport, Alexandria, Egypt*

[4] *Also at Ghent University, Ghent, Belgium*

[5] *Also at Universidade Estadual de Campinas, Campinas, Brazil*

[6] *Also at Federal University of Rio Grande do Sul, Porto Alegre, Brazil*

[7] *Also at UFMS, Nova Andradina, Brazil*

[8] *Also at Nanjing Normal University, Nanjing, China*

[9] *Now at The University of Iowa, Iowa City, Iowa, U.S.A.*

[10] *Also at University of Chinese Academy of Sciences, Beijing, China*

[11] *Also at China Center of Advanced Science and Technology, Beijing, China*

[12] *Also at University of Chinese Academy of Sciences, Beijing, China*

[13] *Also at China Spallation Neutron Source, Guangdong, China*

[14] *Now at Henan Normal University, Xinxiang, China*

[15] *Also at Université Libre de Bruxelles, Bruxelles, Belgium*

[16] *Also at an institute or an international laboratory covered by a cooperation agreement with CERN*

[17] *Also at Cairo University, Cairo, Egypt*

[18] *Also at Suez University, Suez, Egypt*

[19] *Now at British University in Egypt, Cairo, Egypt*

[20] *Also at Purdue University, West Lafayette, Indiana, U.S.A.*

[21] *Also at Université de Haute Alsace, Mulhouse, France*

[22] *Also at Department of Physics, Tsinghua University, Beijing, China*

[23] *Also at Ilia State University, Tbilisi, Georgia*

[24] *Also at The University of the State of Amazonas, Manaus, Brazil*

[25] *Also at Erzincan Binali Yildirim University, Erzincan, Turkey*

[26] *Also at University of Hamburg, Hamburg, Germany*

[27] *Also at RWTH Aachen University, III. Physikalisches Institut A, Aachen, Germany*

[28] *Also at Isfahan University of Technology, Isfahan, Iran*

[29] *Also at Bergische University Wuppertal (BUW), Wuppertal, Germany*

[30] *Also at Brandenburg University of Technology, Cottbus, Germany*

[31] *Also at Forschungszentrum Jülich, Juelich, Germany*

[32] *Also at CERN, European Organization for Nuclear Research, Geneva, Switzerland*

[33] *Also at Institute of Physics, University of Debrecen, Debrecen, Hungary*

[34] *Also at Institute of Nuclear Research ATOMKI, Debrecen, Hungary*

[35] *Now at Universitatea Babes-Bolyai — Facultatea de Fizica, Cluj-Napoca, Romania*

[36] *Also at Physics Department, Faculty of Science, Assiut University, Assiut, Egypt*

[37] *Also at HUN-REN Wigner Research Centre for Physics, Budapest, Hungary*

[38] *Also at Punjab Agricultural University, Ludhiana, India*

[39] *Also at University of Visva-Bharati, Santiniketan, India*

[40] *Also at Indian Institute of Science (IISc), Bangalore, India*

[41] *Also at Birla Institute of Technology, Mesra, Mesra, India*

[42] *Also at IIT Bhubaneswar, Bhubaneswar, India*

[43] *Also at Institute of Physics, Bhubaneswar, India*

[44] *Also at University of Hyderabad, Hyderabad, India*

[45] *Also at Deutsches Elektronen-Synchrotron, Hamburg, Germany*

[46] *Also at Department of Physics, Isfahan University of Technology, Isfahan, Iran*

[47] *Also at Sharif University of Technology, Tehran, Iran*

[48] *Also at Department of Physics, University of Science and Technology of Mazandaran, Behshahr, Iran*

[49] *Also at Helwan University, Cairo, Egypt*

[50] *Also at Italian National Agency for New Technologies, Energy and Sustainable Economic Development, Bologna, Italy*

[51] *Also at Centro Siciliano di Fisica Nucleare e di Struttura Della Materia, Catania, Italy*

[52] *Also at Università degli Studi Guglielmo Marconi, Roma, Italy*

[53] *Also at Scuola Superiore Meridionale, Università di Napoli 'Federico II', Napoli, Italy*

[54] Also at Fermi National Accelerator Laboratory, Batavia, Illinois, U.S.A.

[55] Also at Ain Shams University, Cairo, Egypt

[56] Also at Consiglio Nazionale delle Ricerche — Istituto Officina dei Materiali, Perugia, Italy

[57] Also at Riga Technical University, Riga, Latvia

[58] Also at Department of Applied Physics, Faculty of Science and Technology, Universiti Kebangsaan Malaysia, Bangi, Malaysia

[59] Also at Consejo Nacional de Ciencia y Tecnología, Mexico City, Mexico

[60] Also at Trincomalee Campus, Eastern University, Sri Lanka, Nilaveli, Sri Lanka

[61] Also at Saegis Campus, Nugegoda, Sri Lanka

[62] Also at National and Kapodistrian University of Athens, Athens, Greece

[63] Also at Ecole Polytechnique Fédérale Lausanne, Lausanne, Switzerland

[64] Also at Universität Zürich, Zurich, Switzerland

[65] Also at Stefan Meyer Institute for Subatomic Physics, Vienna, Austria

[66] Also at Laboratoire d'Annecy-le-Vieux de Physique des Particules, IN2P3-CNRS, Annecy-le-Vieux, France

[67] Also at Near East University, Research Center of Experimental Health Science, Mersin, Turkey

[68] Also at Konya Technical University, Konya, Turkey

[69] Also at Izmir Bakircay University, Izmir, Turkey

[70] Also at Adiyaman University, Adiyaman, Turkey

[71] Also at Bozok Universitetesi Rektörlügü, Yozgat, Turkey

[72] Also at Marmara University, Istanbul, Turkey

[73] Also at Milli Savunma University, Istanbul, Turkey

[74] Also at Kafkas University, Kars, Turkey

[75] Now at stanbul Okan University, Istanbul, Turkey

[76] Also at Hacettepe University, Ankara, Turkey

[77] Also at Istanbul University — Cerrahpasa, Faculty of Engineering, Istanbul, Turkey

[78] Also at Yildiz Technical University, Istanbul, Turkey

[79] Also at Vrije Universiteit Brussel, Brussel, Belgium

[80] Also at School of Physics and Astronomy, University of Southampton, Southampton, United Kingdom

[81] Also at University of Bristol, Bristol, United Kingdom

[82] Also at IPPP Durham University, Durham, United Kingdom

[83] Also at Monash University, Faculty of Science, Clayton, Australia

[84] Also at Università di Torino, Torino, Italy

[85] Also at Bethel University, St. Paul, Minnesota, U.S.A.

[86] Also at Karamanoğlu Mehmetbey University, Karaman, Turkey

[87] Also at California Institute of Technology, Pasadena, California, U.S.A.

[88] Also at United States Naval Academy, Annapolis, Maryland, U.S.A.

[89] Also at Bingol University, Bingol, Turkey

[90] Also at Georgian Technical University, Tbilisi, Georgia

[91] Also at Sinop University, Sinop, Turkey

[92] Also at Erciyes University, Kayseri, Turkey

[93] Also at Horia Hulubei National Institute of Physics and Nuclear Engineering (IFIN-HH), Bucharest, Romania

[94] Now at an institute or an international laboratory covered by a cooperation agreement with CERN

[95] Also at Texas A&M University at Qatar, Doha, Qatar

[96] Also at Kyungpook National University, Daegu, Korea

[97] Also at another institute or international laboratory covered by a cooperation agreement with CERN

[98] Also at Universiteit Antwerpen, Antwerpen, Belgium

[99] Also at Yerevan Physics Institute, Yerevan, Armenia

[100] Also at Northeastern University, Boston, Massachusetts, U.S.A.

[101] Also at Imperial College, London, United Kingdom

[102] Also at Institute of Nuclear Physics of the Uzbekistan Academy of Sciences, Tashkent, Uzbekistan